

## Studies of High Temperature Sliding Wear of Metallic Dissimilar Interfaces III: Incoloy MA956 versus Incoloy 800HT

I.A. Inman<sup>\*</sup>, P.S. Datta<sup>a</sup>

*a Northumbria University, Newcastle upon Tyne, NE1 8ST, UK*

---

### Abstract

Wear variations of Incoloy MA956 slid against Incoloy 800HT between room temperature and 750°C, and sliding speeds of 0.314, 0.654 and 0.905 m.s<sup>-1</sup> were investigated using a 'reciprocating-block-on-cylinder' (low debris retention) configuration.

Three forms of wear depending largely on sliding temperature were observed, 'severe wear' with high transfer between room temperature and 270°C, 'severe wear' with low transfer between 390°C and 570°C, and 'glaze' formation' (retarded by increased sliding speed) at 630°C and above. The differences in wear behaviour are discussed, with wear behaviour mapped and wear surfaces at 750°C (0.314 and 0.905 m.s<sup>-1</sup>) cross-sectioned and profiled.

**Keywords:** high temperature, sliding speed, dissimilar materials, wear map

---

### 1. Introduction

'Glaze' layer formation during high temperature 'mild wear' occurs when two metallic surfaces (or a metallic surface versus a suitable ceramic surface) slide against one another under favourable combinations of key tribological parameters, important amongst which are sliding speed, temperature and load. The conditions needed for 'glaze' generation comprehensively studied within AMRI [1-9] and elsewhere [10-32], suggest protective nano-crystalline 'glaze' layer formation under certain conditions (notably higher temperatures), due to a combination of elemental transfer (particularly with dissimilar interface systems), debris generation and oxidation, and also debris sintering [1,2,4,5]. Also, debris' sinterability and thus the readiness with which the 'glaze' is formed can be strongly affected by oxide chemistry [1,5,6].

Lancaster [25], Welsh [26,27], So [28,29] and others [30,31] have shown that various combinations of sliding speed, temperature and load can significantly affect wear behaviour, particularly whether or not a protective 'glaze' forms. Many authors have also constructed wear maps to attempt to present wear data in a simply understood format, allowing prediction of likely wear mode under specified sliding conditions. Lim [33,34], Childs [35] and others [36-43] have constructed wear maps for different sliding systems based on load / pressure and sliding speed. Other wear parameter combinations can also be used, as demonstrated by Kato and Hokkirigawa's abrasive wear map using 'degree of penetration (of asperities)' and 'shear strength at the contact interface' as key parameters [44]. Adachi et al [45] used 'severity of contact' and 'thermal severity of contact' on studying ceramic wear. However, most wear maps have been constructed using room temperature data with little work on elevated temperature sliding (Gómez-del Río et al [43] an exception) or using dissimilar interfaces.

When either Nimonic 80A [1,4,5,7,9] or Incoloy MA 956 were worn against Stellite 6 [6] (both 'dissimilar interface' sliding systems), sliding speed and temperature together affected the preferred

---

\* Corresponding author - E-mail address: [ian@tibet.freeserve.co.uk](mailto:ian@tibet.freeserve.co.uk) (I.A. Inman).

material for wear and also observed wear mode. In both cases, the data collected was used to create simple 'temperature versus sliding speed' wear maps [5,6,7,9].

However, Stellite 6 is an already well established wear-resistant alloy [1- 9, 29, 46-50], its wear properties due partially to a tendency of many Co-based alloys to undergo a shear-induced face-centred cubic to hexagonal-close-packed structural transformation [46-48]. Due to shear-induced alignment of the hexagonal-close-packed basal plane parallel to sliding direction, a thin, easily sheared layer may develop at the sliding surface promoting easy glide [48,49]. This alignment significantly improves galling resistance and reduces friction, with shear and adhesive transfer restricted to this layer; this sliding regime continues even after layer removal as the layer readily regenerates.

Furthermore, material removal in such thin sections may partially explain ready generation of fine Stellite 6-sourced Co-based oxide debris observed in various studies [1,2,5-9,50]. Such sections may be easily commutable to a small size and more readily oxidised, which especially at high temperature potentially provides a ready material supply for wear-protective 'glaze' layer formation.

Both 'face-centred cubic' (Incoloy 800HT) and 'body-centred cubic' (Incoloy MA956) systems in contrast have 12 primary slip systems available [51,52]. Furthermore, in body-centred cubic structures, raising temperature [51] or shear stress [52] may increase the number of active slip systems; an extra 10% shear stress may allow slip on a further 36 systems [52]. Such alloys normally have poor galling resistance compared to cobalt-based alloys; heavy deformation and metallic debris generation (i.e. severe wear) can be expected [46]. Indeed, there is potential for mechanical alloying where metallic debris from both sliding surfaces is mixed together and redeposited on either or both wear surfaces [53-55].

However, Incoloy MA956-sourced Fe-Cr-based oxides can themselves readily form 'glaze' layers [6]. The current study examines whether such 'glaze' layers formed at higher temperature can protect potentially highly deformable 'commercial' alloys. Brief comment is also made of the possible effect of second phases within these alloys, used to improved mechanical and high temperature properties. Incoloy MA956 is an oxide dispersion strengthened (ODS) alloy with monoclinic ( $3Y_2O_3 \cdot 5Al_2O_3$ ) and tetragonal ( $2Y_2O_3 \cdot Al_2O_3$ ) precipitates of size between 3 and 60 nm [56]. Incoloy 800HT contains a fine dispersion of titanium nitrides, titanium carbides and chromium carbides of between 1  $\mu m$  and 3  $\mu m$  [57].

Additionally, EDX profiling of the surface layers generated (at 750°C, and sliding speeds of 0.314 and 0.905  $m \cdot s^{-1}$ ) is used to establish a probable order of deformation and layer-formation events from the start of sliding through to final 'glaze' layer generation.

## 2. Experimental

### 2.1 Temperature versus Sliding Speed Study

The alloy compositions used in this study are detailed in Table 1.

The tests were carried out using a high temperature ‘reciprocating-block-on-rotating-cylinder’ wear rig (Incoloy MA965 blocks forming the samples and an Incoloy 800HT cylinder, the counterface) in air (Fig. 1). The configuration used was such that debris retention was not encouraged. The counterface, diameter 50 mm and length 50 mm, was mounted on a shaft rotated by a variable speed electric motor. Individual ‘block’ samples, 5 mm x 5 mm x 45 mm (acetone cleaned after polishing to a 1  $\mu\text{m}$  surface finish) were held against the counterface (acetone cleaned after polishing to a 1200 grit finish), using a sample arm in reciprocating motion with a constant stroke of 12 mm, at 3 cycles per minute. The tests were carried out at sliding speeds of 0.314, 0.654 and 0.905  $\text{m}\cdot\text{s}^{-1}$ , under 7N load at room temperature (R.T.), 270, 390, 450, 510, 570, 630, 690 and 750°C. The total sliding distance for all tests was 4,522 m.

A minimum of three tests (one per sample) were conducted for each combination of conditions. Each Incoloy MA956 sample was weighed using a high accuracy Sartorius microbalance before and after sliding, from which each set of sliding conditions’ mean weight change was calculated; weight loss was recorded as a negative value. Wear of the Incoloy 800HT counterface was not assessed quantitatively in the current study. The coefficient of friction data were collected by a Melbourne type TRP-50 torque transducer connected to the rotating counterface shaft.

The microstructures (primarily at 0.314 and 0.905  $\text{m}\cdot\text{s}^{-1}$ ) were characterised at micro-scale level using Scanning Electron Microscopy (SEM), Energy Dispersive X-ray (EDX – data in wt%) and X-ray Diffraction (XRD). The SEM (a Hitachi SM2400) was also used to collect EDX and Autopoint EDX data. A Siemens Diffraktometer 5000 was used to collect XRD data with a locked detector tube between ‘ $2\theta$ ’ angles of 10 to 90° (‘ $\theta$ ’ the angle of incidence of the X-rays) and a Cu  $K\alpha$  source. This XRD data was interpreted using the associated *DIFAC-DOS/DIFAC+* software and diffraction pattern database, to determine the phases present on the wear scar.

The weight change data and observations made were used to construct a simple temperature versus sliding speed wear map for the Incoloy MA956 (sample) versus Incoloy 800HT (counterface) combination. Data previously presented by Rose [9] for 0.654  $\text{m}\cdot\text{s}^{-1}$ , allowed emphasis on 0.314 and 0.905  $\text{m}\cdot\text{s}^{-1}$  in the current study. 0.654  $\text{m}\cdot\text{s}^{-1}$  sliding tests were repeated, however, to ensure observations matched with the shorter 4,522 m sliding distance used in the current study (Roses’ data [9] was collected after 9,418 m of sliding) and collect weight change data for wear map development. The following data and discussion concentrates on sample wear behaviour. Counterface EDX analysis is reported at 750°C only, due to difficulties sectioning suitable samples and a need to reuse counterfaces for continued testing.

## 2.2 Characterisation of Evolved Layers at 750°C

Samples slid at 0.314 and 0.905 m.s<sup>-1</sup> were cross-sectioned, after which the cross-sections underwent SEM study and profiled using a system called 'Autopoint'. In other words, EDX was done at regular intervals through a cross-section, starting at the worn surface and passing through the wear-affected layers into the undeformed substrate. Such analysis helped determine effects such as degree of transfer, mixing of sample and counterface material and preferential elemental diffusion. The information was used to predict a probable order of events during the sliding process.

## 3. Results

### 3.1 Weight Change and Friction Data

#### 3.1.1 0.314 m.s<sup>-1</sup>

At 0.314 m.s<sup>-1</sup>, weight change values (Fig. 2) indicated at first a gradual but later accelerating rise in Incoloy MA956 weight loss with increasing temperature (mean weight change -0.002(9) g at R.T., -0.151(6) g at 510°C), with large jumps in weight loss notably at 630°C (-0.202(7) g) and 690°C (-0.282(6) g). A decrease in weight loss was observed at 750°C (-0.090(3) g).

Coefficient of friction values for the Incoloy MA956 / Incoloy 800HT system at 0.314 m.s<sup>-1</sup> showed two distinct phases of behaviour (Fig. 3), a pattern repeated at 0.654 and 0.905 m.s<sup>-1</sup>. An initial unsettled 'run-in' period (typical frictional variation ~20%) lasted up to ~1,000 m of sliding, followed by a more settled 'steady state' period (a reduced ~12% variation) up to the end of testing.

Whilst there was no clear temperature-related trend in early peak 'run-in' coefficient of friction values (reaching to between 1 and 1.2 regardless of sliding speed – Fig. 3), a downward trend in 'steady state' values was observed, falling from between 0.75 - 0.85 at R.T., to 0.6 - 0.75 at 270°C, 0.58 - 0.67 at 450°C, 0.6 - 0.7 at 510°C and finally 0.4 - 0.6 between 630°C - 750°C.

The 0.314 m.s<sup>-1</sup> coefficient of friction data at 'glaze' forming temperatures (630°C to 750°C) also showed a change from more to less variable values during 'steady state' sliding from ~12 to ~8%, coinciding with substantial 'glaze' formation reducing 'metal-to-metal' contact [2]. This occurred earlier with increasing temperature (Fig. 3); after ~2,920 m of sliding at 630°C, ~3,062 m at 690°C and ~1,036 m at 750°C.

#### 3.1.2 0.654 m.s<sup>-1</sup>

Observed wear behaviour at 0.654 m.s<sup>-1</sup> followed a very similar pattern to that at 0.314 m.s<sup>-1</sup> (Fig. 2). There was a gradual increase in weight loss between room temperature (negligible weight change) and 510°C (-0.0459(4) g), this accelerating up to 630°C (-0.132(2) g). There was a large jump in weight loss at 690°C (-0.322(7) g) followed by a limited decrease at 750°C (-0.298(4) g).

At  $0.654 \text{ m.s}^{-1}$ , the unsettled 'run-in' period of coefficient of friction (Fig. 4) lasted for the first  $\sim 1,000 \text{ m}$  of sliding (variation  $\sim 20\%$ ), before the 'steady state' period was established (variation  $\sim 12\%$ , though at  $750^\circ\text{C}$  it was  $\sim 20\%$  – the reason for this could not be identified).

There was no obvious trend in early peak 'run-in' coefficient of friction with increasing sliding temperature (Fig. 5), however, there was a downward trend in 'steady state' values, falling from between 0.7 and 0.75 at R.T., to 0.62 - 0.67 at  $270^\circ\text{C}$ , 0.65 - 0.72 at  $450^\circ\text{C}$ , 0.64 - 0.71 at  $510^\circ\text{C}$  and finally 0.45 - 0.55 at  $750^\circ\text{C}$ . The  $0.654 \text{ m.s}^{-1}$  situation was very similar to that at  $0.314 \text{ m.s}^{-1}$ .

A change from more to less variable coefficient of friction from  $\sim 12\%$  to  $\sim 8\%$  coinciding with 'glaze' layer formation [2], was only observed at  $690^\circ\text{C}$  after  $\sim 1,908 \text{ m}$  and  $750^\circ\text{C}$  after  $\sim 1507 \text{ m}$ . No such change was observed at  $630^\circ\text{C}$ , suggesting the very limited oxidation was insufficient to eliminate 'metal-to-metal' contact before the end of testing.

### **3.1.3 $0.905 \text{ m.s}^{-1}$**

Between R.T. and  $630^\circ\text{C}$ , the pattern of wear behaviour at  $0.905 \text{ m.s}^{-1}$  followed a pattern similar to that at  $0.314$  and  $0.654 \text{ m.s}^{-1}$  (Fig. 2), with at first a gradual (mean weight change  $-0.004(7) \text{ g}$  at R.T.,  $-0.062(0) \text{ g}$  at  $510^\circ\text{C}$ ) but accelerating increase in weight loss ( $-0.131(2) \text{ g}$  at  $630^\circ\text{C}$ ). Additionally, lower weight change was observed at  $0.905 \text{ m.s}^{-1}$  than at  $0.314 \text{ m.s}^{-1}$  between  $390^\circ\text{C}$  and  $630^\circ\text{C}$ . However, weight loss continued to rise at  $0.905 \text{ m.s}^{-1}$  on increasing temperature to  $690^\circ\text{C}$  ( $-0.257(6) \text{ g}$ ) and (unlike  $0.314$  and  $0.654 \text{ m.s}^{-1}$ )  $750^\circ\text{C}$  ( $-0.332(0) \text{ g}$ ).

Variations in coefficient of friction for the Incoloy MA956 / Incoloy 800HT system at  $0.905 \text{ m.s}^{-1}$  (Fig. 5) were typically as high as  $\sim 30\%$  during the unsettled 'run-in' phase and  $\sim 20\%$  during 'steady state'. This compared to corresponding values of  $\sim 20\%$  and  $\sim 12\%$  at both  $0.314$  and  $0.654 \text{ m.s}^{-1}$ .

No clear trend in peak 'run-in' coefficient of friction values presented itself with respect to temperature (Fig. 5). Also no trend was obvious either during 'steady-state' sliding (unlike  $0.314$  and  $0.654 \text{ m.s}^{-1}$ ), however, coefficient of friction at  $750^\circ\text{C}$  was substantially lower (between 0.4 - 0.55 at  $750^\circ\text{C}$ , compared to 0.58 - 0.72 at R.T. and  $270^\circ\text{C}$ , 0.7 - 0.8 at  $450^\circ\text{C}$  and 0.65 - 0.82 at  $510^\circ\text{C}$ ). The higher variation and lack of clear trends in frictional data at  $0.905 \text{ m.s}^{-1}$ , may be due to increased equipment vibration at this higher sliding speed.

The change from more to less variable coefficient of friction values during steady state sliding noted at  $0.314 \text{ m.s}^{-1}$  ( $630$ ,  $690$  and  $750^\circ\text{C}$ ) and  $0.654 \text{ m.s}^{-1}$  ( $690$  and  $750^\circ\text{C}$ ), was observed only at  $750^\circ\text{C}$  after  $\sim 2,285 \text{ m}$  sliding at  $0.905 \text{ m.s}^{-1}$ . Only at  $750^\circ\text{C}$  was there apparently sufficient 'glaze' development to eliminate metal-to-metal contact within  $4,522 \text{ m}$  at  $0.905 \text{ m.s}^{-1}$ . Elimination of metallic contact was only achievable at  $630$  and  $690^\circ\text{C}$  by increasing test sliding distance [1].

### 3.2 Wear Scar Morphology

Optical and SEM examination (Figs. 6, 7, 8 and 9) indicated that at R.T. and 270°C, Incoloy MA956 sample wear surfaces were metallic and highly damaged (indicative of severe wear), with extensive metallic transfer onto the Incoloy MA956 surface at 0.314, 0.654 (not shown) and 0.905 m.s<sup>-1</sup>. The resulting metallic transfer layer covered almost the entire wear scar, coinciding with fairly low weight loss at these temperatures. Confirmation of which was transfer layer and which was exposed substrate (and thus level of coverage) was made by spot EDX analysis (Section 3.3.1), possible due to changes in composition from mechanical alloying.

Transfer levels at all three sliding speeds were much lower at temperatures of 390°C and above. The decreasing transfer was accompanied by increasing discolouration due to very limited oxidation of the exposed metallic surfaces (Figs. 6 and 7 – this oxidation, though sufficient to cause an increase in metallic discolouration, did not build up into wear-protective oxide layers), coinciding with increasing sample weight loss. At 0.314 m.s<sup>-1</sup>, only isolated areas of transferred metallic material were deposited on the wear scar surfaces covering at most ~5 to 10% of their area. Metallic transfer at 0.654 and 0.905 m.s<sup>-1</sup> was slightly higher, though the patchy metallic transfer layers formed were still limited to ~50% of the wear scar; this greater transfer may explain the apparent reduced weight change values at 0.905 m.s<sup>-1</sup> (compared to 0.314 m.s<sup>-1</sup>) seen between 390 and 630°C. There was no clear evidence of this oxide modifying or further enhancing wear by abrasion at any sliding speed (a highly damaged, metallic surface persisted with no apparent polishing effect), though some abrasive effect cannot be discounted.

‘Glaze’ formation and ‘mild wear’ at 0.314 was first observed at 630°C (Figs. 6 and 8), covering approximately 70% of the wear scar. The ‘glaze’ layers became more comprehensive with 90% wear scar coverage on increasing sliding temperature to 690°C and 750°C (Figs. 6 and 8); the arrest in increasing weight loss at 750°C was observed alongside this.

At 0.654 and 0.905 m.s<sup>-1</sup>, ‘glaze’-type layers on the Incoloy MA956 samples first appeared at 630°C (Fig. 7 shows the 0.905 m.s<sup>-1</sup> example), but only in limited patches. Oxide layer formation increased with temperature and at 0.654 m.s<sup>-1</sup>, patchy ‘glaze’ layers were observed at 690°C; there was comprehensive ‘glaze’ coverage at 750°C, coinciding again with weight loss being arrested. However, oxide layer formation was suppressed at 0.905 m.s<sup>-1</sup> with still patchy ‘glaze’ formation at 690°C. There was no more than 40 to 50% ‘glaze’ coverage at 750°C (though sufficient to allow cross-sectional analysis – Figs. 7 to 9), with no accompanying arrest in weight loss.

Other studies [1] showed that extended sliding was required at 0.905 m.s<sup>-1</sup> (up to 13,032 m at 750°C) to form comprehensive ‘glaze’ layers and fully establish mild wear. Some fracturing of the ‘glaze’ was observed at all three sliding speeds and especially 0.905 m.s<sup>-1</sup> (Fig. 9). There were no signs of the oxide in loose form having a significant abrasive effect between 630 and 750°C (as would be

evidenced by the formation of fine, parallel grooves on the wear scar [1, 4, 5, 7]), with it either forming 'glaze', being ejected or collecting (at 690 and 750°C) in the counterface wear track.

Atomic Force Microscopy (AFM) [58] indicated a minimum 'glaze' layer grain size of ~25 nm for 750°C samples slid at 0.314 and 0.905 m.s<sup>-1</sup> (Fig. 10); finer structures were possible but they could not be 'resolved'.

At 690 and 750°C, there was evidence of material softening and plastic deformation of the Incoloy MA956, the clearest indication being 'rims' of material pushed out from the sides of the wear interface. These were most apparent at 750°C and 0.905 m.s<sup>-1</sup> (Fig. 7).

### **3.2.1 Debris Morphology**

The large flat platelet-type metallic debris particles typical of delamination wear (Figs. 11 and 12), were produced at all three sliding speeds over the entire range of test temperatures (R.T. to 750°C); particle sizes ranged between 20 µm and 1 mm. No oxide was present amongst this metallic debris at R.T. and 270°C. At 390°C, 450°C, 510°C and 570°C, some oxide debris was observed, but only in trace amounts amongst the overwhelmingly metallic debris; this coincided with the discolouration of wear scar surfaces due to very limited oxidation at these temperatures. Further evidence of limited oxidation (insufficient to form oxide layers) was hinted at during SEM by charging on the metallic debris surfaces at 510°C (Fig. 11) and 0.314 m.s<sup>-1</sup> during SEM.

Significant levels of oxide debris were only apparent amongst the metallic debris at 630°C and above, coinciding with the beginning of 'glaze' layer formation; this oxide debris was of size between ~300 nm and ~1 µm. Levels of oxide debris produced increased with temperature between 630°C and 750°C, however, the larger, flattened platelet-like metallic debris (of size 20 µm to 1 mm) were also still present (Figs. 11 and 12).

### **3.2.2 Incoloy 800HT Counterface Wear Scar Morphology**

Severe wear of the Incoloy 800HT counterface was observed at 0.314, 0.654 and 0.905 m.s<sup>-1</sup> throughout the range of test temperatures, with observations almost identical regardless of sliding speed (Fig. 13a shows examples from 0.314 m.s<sup>-1</sup>). Between R.T. and 450°C, the counterface wear scar was highly worn with a limited metallic transfer layer forming upon it, due to transfer and back-transfer between the Incoloy MA956 sample and the counterface. A reduction in this layer was observed at 390°C and 450°C (mirroring sample behaviour), coinciding with wear surface discoloration due to limited oxidation.

At 510°C and above, the Incoloy 800HT counterface wear track formed a deep, heavily worn 1.5 mm deep groove (Fig. 13b) and from 570°C upwards, asperities appeared within this wear track (slightly fewer at 0.905 m.s<sup>-1</sup>). The asperities reached heights of up to 1.5 mm above the unworn

counterface and can only have been formed from redeposition of removed material. 'Glaze' formed at 690 and 750°C at all three sliding speeds, but only on asperity peaks; this matched the increased oxide layer formation on the Incoloy MA956 wear surfaces at these temperatures. This 'glaze' can only have formed after the asperities, indicating early counterface 'severe wear' before 'mild wear' was established.

Large quantities of easily dislodged loose oxide debris generated during the wear process also lay in the counterface wear track at 690 and 750°C at all three sliding speeds.

### **3.3 EDX Analysis**

#### **3.3.1 Sample Surface**

For samples slid at both 0.314 and 0.905 m.s<sup>-1</sup> (R.T. and 270°C), EDX analysis clearly indicated metallic transfer from the Incoloy 800HT counterface and mixing with Incoloy MA956 sample material (at R.T., 18% Ni, 29% Cr and 47% Fe at 0.314 m.s<sup>-1</sup> and ~19% Ni, ~29% Cr and ~43% Fe at 0.905 m.s<sup>-1</sup>; similar at 270°C). A 'mechanically mixed / alloyed' metallic transfer layer resulted overlying the Incoloy MA956 surface, of intermediate composition between sample and counterface. However, a still highly variable composition (some areas were close to either the Incoloy MA956 or Incoloy 800HT) indicated mixing was incomplete. There were no signs of enhanced mixing by sliding speed.

For samples slid at 0.314 m.s<sup>-1</sup> between 390°C and 570°C, there was a reduction in Ni to ~10% in remaining areas of transferred metallic material, showing less Incoloy 800HT contribution. At 0.905 m.s<sup>-1</sup>, there was no more than 3% Ni in deposited material, indicating even less Incoloy 800HT contribution than at 0.314 m.s<sup>-1</sup> (with Fe at 60% and Cr at 27%); similar data was obtained on samples slid up to 630°C. At both sliding speeds (especially 0.905 m.s<sup>-1</sup>), most adhered material was redeposited Incoloy MA956. The remaining largely transfer layer-free areas of sample wear scar (indicated by an absence of significant Ni) also gave values consistent with Incoloy MA956.

'Glaze' layers formed at 630°C and above (0.314 and 0.905 m.s<sup>-1</sup>) gave proportions of Cr (26-28% at 0.314 m.s<sup>-1</sup>; 23-27% at 0.905 m.s<sup>-1</sup>) and Fe (60-62% at 0.314 m.s<sup>-1</sup>; 67-68% at 0.905 m.s<sup>-1</sup>) consistent with Incoloy MA956, showing the oxidised 'glaze' material to be almost entirely Incoloy MA956-sourced. Only slight traces of Incoloy 800HT-sourced Ni (0-3% at 0.314 m.s<sup>-1</sup>; 0.5-1% at 0.905 m.s<sup>-1</sup>) indicated that increasing sliding speed to 0.905 m.s<sup>-1</sup> did not encourage extra transfer from the Incoloy 800HT. All levels within the 'glaze' layers between 630°C and 750°C were higher than expected, at around ~7.5% for 0.314 m.s<sup>-1</sup> and 8-11% for 0.905 m.s<sup>-1</sup> compared to ~4.5% within unworn Incoloy MA956.



### 3.3.2 Debris

At both 0.314 m.s<sup>-1</sup> and 0.905 m.s<sup>-1</sup>, analysis of metallic debris formed between R.T. and 390°C gave mixed results, with composition varying between that of Incoloy MA956 and of Incoloy 800HT depending on selected debris particle. With debris formed at 390°C and 450°C, the composition normally matched Incoloy MA956 coinciding with reduced Incoloy 800HT transfer at these temperatures, Incoloy MA956 remained the almost exclusive source of metallic debris between 510°C and 750°C. Fe in the metallic debris varied between ~59% and ~67%, Cr between ~23% and ~28%, Al between ~5% and ~10%, with Ni never exceeding 2.5%. As Ni was only present in the Incoloy 800HT counterface, the data showed little Incoloy 800HT contribution to the debris between 390°C and 750°C.

The Incoloy MA956 sample was also the near exclusive source for the loose oxide debris generated at both 0.314 m.s<sup>-1</sup> and 0.905 m.s<sup>-1</sup> for temperatures of 630°C, 690°C and 750°C (where sufficient oxide debris was available for analysis); levels of Fe, Cr and Ni were close to those for the metallic debris and unworn Incoloy MA956. This applied to both the ejected oxide debris and that in the bottom of the Incoloy 800HT counterface wear track.

### 3.3.3 Counterface Surface (750°C)

The 'glaze' forming on the Incoloy 800HT counterface wear track asperities at 750°C, was of intermediate composition between the counterface and the Incoloy MA956 sample (0.314 and 0.905 m.s<sup>-1</sup>). Counterface 'glaze' formed at 0.314 m.s<sup>-1</sup> had a mean composition of ~18% Ni, 20% Cr and 58% Fe. That formed at 0.905 m.s<sup>-1</sup> gave results of ~16% Ni, ~21% Cr and ~58% Fe.

The asperities could not be analysed, due to the aforementioned difficulties with sectioning and the need to reuse the counterfaces for further testing (sectioning would have destroyed the counterfaces).

### 3.3.4 Previous Data

Previously slid 0.654 m.s<sup>-1</sup> samples and associated debris [9] gave EDX values concurring with those seen at 0.314 and 0.905 m.s<sup>-1</sup> in the current study.

## 3.4 XRD Analysis

XRD analysis (Table 2) indicated the presence of Fe-Cr in all cases regardless of sliding speed or temperature, consistent with the Incoloy MA956 sample. However, the presence of other phases depended strongly on temperature and less so on sliding speed, giving three distinct sets of results.

At R.T. and 270°C, Fe-Cr and also Ni-containing Cr<sub>0.19</sub>Fe<sub>0.7</sub>Ni<sub>0.11</sub> phases were detected; this latter phase indicated transfer from the Incoloy 800HT counterface. This corresponds with EDX-indicated mixed composition transfer layer development on the Incoloy MA956 sample at these

temperatures. For Incoloy 800HT,  $\text{Ni}_{2.9}\text{Cr}_{0.7}\text{Fe}_{0.36}$  was the more normally obtained Ni-containing phase; the reduced Ni-containing  $\text{Cr}_{0.19}\text{Fe}_{0.7}\text{Ni}_{0.11}$  phase further indicates mechanical alloying.

From 390°C up to the start of ‘glaze’ formation at 630°C, only Fe-Cr was detected without a signal for  $\text{Cr}_{0.19}\text{Fe}_{0.7}\text{Ni}_{0.11}$ . This corresponds to reduced material transfer and loss of the transfer layer on the Incoloy MA956. The remaining Ni detected by EDX (in reduced patches of transfer) appears insufficient for XRD phase detection.

$\text{Cr}_{1.3}\text{Fe}_{0.7}\text{O}_3$  was detected from 510°C upwards on the 0.314  $\text{m}\cdot\text{s}^{-1}$  Incoloy MA956 wear scar surfaces (despite no oxide layers at 510°C and 570°C). This coincided with slight charging due to the limited oxide observed on the debris during SEM (Fig. 11). The  $\text{Cr}_{1.3}\text{Fe}_{0.7}\text{O}_3$  signal was stronger at ‘glaze’ forming temperatures (630°C, 690°C and 750°C).

XRD analysis did not detect any oxide phase on the 0.654 and 0.905  $\text{m}\cdot\text{s}^{-1}$  samples slid at 510 and 570°C, and additionally (despite isolated patches of ‘glaze’) for 0.905  $\text{m}\cdot\text{s}^{-1}$  samples slid at 630°C. This is despite increasing oxidation-induced discolouration between 390°C and 630°C.  $\text{Cr}_{1.3}\text{Fe}_{0.7}\text{O}_3$  was only detected at both higher sliding speeds once oxide layers started developing at 630, 690°C and 750°C; no Ni-containing phase was detected. Increasing sliding speed did not result in ‘glaze’ layer oxide phase changes, which continued to be primarily Incoloy MA956-sourced.

### 3.5 Micro-hardness Testing of Transfer and ‘Glaze’ Layers

The mean hardness of transfer layers formed on the Incoloy MA956 samples (Table 3) at R.T. (5.82 GPa at 0.314 $\text{m}\cdot\text{s}^{-1}$ , 6.72 GPa at 0.905  $\text{m}\cdot\text{s}^{-1}$ ) and 270°C (7.11 GPa at 0.314  $\text{m}\cdot\text{s}^{-1}$ , 6.10 GPa at 0.905  $\text{m}\cdot\text{s}^{-1}$ ) were consistently higher than either the undeformed Incoloy MA956 substrate (4.129 GPa) or the Incoloy 800HT counterface (2.15 GPa). These transfer layers thus show significant work-hardening.

Due to the absence or patchiness of metallic transfer layers on either the 0.314  $\text{m}\cdot\text{s}^{-1}$  or 0.905  $\text{m}\cdot\text{s}^{-1}$  samples at temperatures >270°C, no viable data was obtainable.

There was a large difference in apparent comprehensive ‘glaze’ layer hardness for the 750°C samples with sliding speed, with average values of 9.6 GPa at 0.314  $\text{m}\cdot\text{s}^{-1}$  and 21.3 GPa at 0.905  $\text{m}\cdot\text{s}^{-1}$  (Table 4). There was no collapse of ‘glaze’ layers overlying the Incoloy MA956 during hardness testing, with no loose powdery layer between ‘glaze’ and sample metal as with other combinations [1,6]. However, there were wide location-dependent variations in measured ‘glaze’ hardness, probably due to the indenter penetrating the at times very thin ‘glaze’ layer into the underlying material (lower hardness values were obtained in such cases). These variances suggest caution with apparent differences in hardness between layers formed at 0.314 and 0.905  $\text{m}\cdot\text{s}^{-1}$ .

Cross-sectional profiling (reported elsewhere [1]) did not indicate substantial hardening of sub-surface layers at either 0.314 or 0.905 m.s<sup>-1</sup>.

Testing of 0.654 m.s<sup>-1</sup> samples during previous studies [9] also indicated hardening close to the surface. However, no hardness data was obtained for 'glaze' layers formed at 0.654 m.s<sup>-1</sup> [9].

### **3.6 Cross-sectional Autopoint EDX Analysis of 'Glaze' Layers at 750°C**

#### **3.6.1 0.314 m.s<sup>-1</sup>**

A two-layer structure was observed on all 0.314 m.s<sup>-1</sup> samples examined (Fig. 14), consisting of a 'glaze' layer of no more than 2 µm thickness and a mixed metal-oxide layer, extending usually to between 15 to 20 µm depth (17 to 18 µm in the discussed example). However, localised reduced removal from the Incoloy MA956 sample material during early severe wear has led to the intermediate mixed metal-oxide layer deposited following being much thinner in some locations; Fig.13 demonstrates one such area where the mixed metal-oxide layer is only 3 to 4 µm thick. Incoloy 800HT-sourced Ni levels were negligible (~0.3%) in the 'glaze' and debris layers; the Incoloy MA956 was thus the near-exclusive source for the 'glaze' and mixed metal-oxide debris, which consisted of Fe, Cr, Al and trace Si (~1.4% max.).

Fe, Cr and Al levels were extremely variable implying diffusion within the mixed metal-oxide debris layer, with the highest Cr concentrations occurring where there were Fe minima and vice versa (Fig. 14). Starting at the debris / Incoloy MA956 substrate interface at 17 µm depth and moving up towards the surface 'glaze' layers:

- at the interface between the debris and the Incoloy MA956 substrate, Fe accounted for ~63% of the metallic content and Cr accounted for ~28% (i.e. typical Incoloy MA956 composition);
- at 14 µm depth, an Fe minimum was encountered, matching a Cr peak (~40% Fe, ~50% Cr);
- at 10 µm, Fe recovered to a peak at which point Cr was at a minimum (Fe ~71%, Cr ~18%);
- Fe fell to a further minimum at 4 µm depth, coincident with another mini-peak in Cr (Fe ~55%, Cr ~32%).

Between the debris / Incoloy MA956 interface and ~6 µm depth, Al levels showed some variation but remained low. However, between 4 to 6 µm depth and the surface (irrespective of sample analysed) Al levels rose sharply. In the Fig. 14 example, Al rose from ~8% at 6 µm depth to ~22% in isolated areas of the 'glaze' surface (though maximum values were normally no greater than ~12%). Over the same distance, both Fe levels (from ~55 to ~52%) and in particular Cr levels (from 32 to 22%) fell as Al content increased. Composition values in other samples were similar, falling into a band 2 to 3% at either side of those in Fig. 14.

There was no clear trend at  $0.314 \text{ m.s}^{-1}$  regarding the Fe / Cr / Al data with respect to O content within the mixed metal-oxide layer, with O levels increasing erratically from the Incoloy MA956 substrate / debris interface towards the debris surface (although an O peak at  $10 \mu\text{m}$  depth – 58% of the overall content – coincided with the metallic content maximum for Fe of 71%). However, the highest O concentrations (~78% of overall content) matched those for Al at the ‘glaze’ surface. Al has diffused towards the surface and oxidised in preference to Fe and especially Cr.

The Incoloy 800HT counterface contains only trace Al and thus its presence cannot be accounted for by transfer to the Incoloy MA956 surface.

### **3.6.2 $0.905 \text{ m.s}^{-1}$**

Increasing sliding speed to  $0.905 \text{ m.s}^{-1}$  ( $750^\circ\text{C}$ ) resulted in a similar but thinner multi-layer structure (7 to  $12 \mu\text{m}$  thickness – Fig. 15) to that at  $0.314 \text{ m.s}^{-1}$  (15 to  $20 \mu\text{m}$  thickness); however, this could locally vary as at  $0.314 \text{ m.s}^{-1}$ . The multi-layer structure consisted of a mixed metal-oxide debris layer lying between  $1.5 \mu\text{m}$  depth and the Incoloy MA956 / debris interface at 7 to  $12 \mu\text{m}$  depth (~ $9 \mu\text{m}$  in the discussed example – Fig. 15), overlaid by a ‘glaze’ layer of 1 to  $1.5 \mu\text{m}$  maximum thickness. The mixed debris layer was completely oxidised between  $1.5$  and  $5 \mu\text{m}$  depth, this material forming an extra distinct sub-layer beneath the ‘glaze’.

At  $0.905 \text{ m.s}^{-1}$ , negligible Ni in the ‘glaze’ or debris layers indicated little Incoloy 800HT counterface contribution. The dominance of Fe, Cr and Al, with trace silicon (~1.25%) indicated that Incoloy MA956 was the near exclusive debris source. Within the mixed debris layer (starting at ~ $9 \mu\text{m}$  depth), Fe, Cr and Al levels were highly erratic, the Fe minima coinciding with peaks of either Al (at  $7.5 \mu\text{m}$  depth – Fe 40%, Al 32%) or Cr (at  $6 \mu\text{m}$  depth – Fe 42%, Cr 40%).

Unlike  $0.314 \text{ m.s}^{-1}$ , there was some match at  $0.905 \text{ m.s}^{-1}$  between Fe and O level variation in the ‘glaze’ and mixed debris layers, with Fe peaks coincident with O minima and vice versa. This was most noticeable towards the surface; in Fig. 15 at  $5 \mu\text{m}$  depth, the Fe peak of 72% of metallic content matched a large fall in overall O content to 28%. Closer to the surface, Fe’s share of the metallic content decreased to 43% as Al’s share of the metallic content increased to 32% and O’s share of the overall content increased to 82%. Preferential diffusion towards and oxidation of Al at the ‘glaze’ surface was again apparent.

Cr levels remained fairly constant through both oxide debris and ‘glaze’ layers at 20 to 22% of the metallic content. There was no relevant variation in other element levels.

#### 4. Wear Map for Incoloy MA956 versus Incoloy 800HT

Using the information presented, it is possible to construct the following wear map for Incoloy MA956 worn against Incoloy 800HT (Fig. 16), describing wear behaviour as a function of sliding speed and temperature. Three main regions of different wear behaviour are shown:

1. A 'severe wear' mechanism dominated at R.T. and 270°C, with extensive metallic transfer between the Incoloy MA956 and the Incoloy 800HT. A mixed, work-hardened metallic transfer layer formed, protecting the Incoloy MA956 from continued wear.
2. Severe wear continued, but with much reduced metallic transfer up to 570°C. The lack of a protective transfer layer resulted in greater Incoloy MA956 wear. Adhesion was inhibited due to surface oxidation (observable as wear surface discolouration), detectable by XRD on 0.314 m.s<sup>-1</sup> samples slid at 510 and 570°C. There was greater metallic transfer layer build-up and less wear at 0.654 and 0.905 m.s<sup>-1</sup>, due to enhanced removal of surface oxidation.
3. 'Glaze' formation (the oxide Incoloy MA956-sourced) and 'mild wear' occurred between 630°C and 750°C, preceded by a period of 'severe wear' with limited transfer. However, the readiness with which the 'glaze' formed and its protective abilities were reduced by higher sliding speed extending initial 'severe wear' and enhancing debris ejection.
  - a. At 0.314 m.s<sup>-1</sup>, comprehensive 'glaze' formation (the oxide Incoloy MA956-sourced) occurred between 630°C and 750°C, preceded by a period of 'severe wear' with limited transfer. This 'glaze' formed rapidly enough to reduce overall wear only at 750°C.
  - b. At 0.654 m.s<sup>-1</sup>, there was some 'glaze' development on the wear scar surface at 630°C. More complete 'glaze' layers formed after increased 'severe wear' at 690°C and 750°C (compared to that at 0.314 m.s<sup>-1</sup>), the oxide for these layers Incoloy MA956-sourced. Rapid development of these 'glaze' layers again reduced wear only at 750°C.
  - c. At 0.905 m.s<sup>-1</sup>, 'glaze' formation was extremely limited at 630°C. Patchy 'glaze' formation occurred at 690°C and an incomplete 'glaze' at 750°C, however, neither prevented continued increased wear within the set 4,522 m sliding distance due to delayed formation and the 'severe wear' period was extended further. The oxide in all cases remained Incoloy MA956-sourced. Incoloy MA956 softening and plastic deformation might have also reduced support for the 'glaze'.

Greater 'glaze layer development was only apparent at 0.905 m.s<sup>-1</sup> after 13,032 m of sliding [1].

## 5. Discussion

### 5.1 General Studies

The wear of Incoloy MA956 (sample) against Incoloy 800HT (counterface) at all three sliding speeds, showed three distinct wear regimes between R.T. and 750°C.

#### 5.1.1 Room Temperature and 270°C

At R.T. and 270°C (Fig. 16, Region 1), moderate amounts of flattened metallic wear debris (Figs. 11 and 12) were produced by a standard ‘severe wear’ delamination-type mechanism from both the Incoloy MA956 sample and Incoloy 800HT counterface. Much of this metallic debris readhered to either the sample or counterface, forming a mechanically mixed metallic transfer layer (Figs. 6 to 9), which became work hardened due to sliding (Table 3) and limited the amount of wear (Fig. 2). The mechanical mixing producing this layer was incomplete (i.e. heterogeneous), demonstrated by variable levels of Ni, Cr and Fe and the reduced Ni-containing  $\text{Cr}_{0.19}\text{Fe}_{0.7}\text{Ni}_{0.11}$  phase detected during XRD. The absence of oxide from either sliding surface at R.T. and 270°C indicated oxidation played no significant part in the wear process, either to protect the wear surfaces from high wear (as was the case with Incoloy MA956 versus Stellite 6 [6]) or to inhibit adhesion and transfer layer build-up on either surface.

Visual monitoring at R.T. suggested continued metallic removal from and deposition onto both sample and counterface, with readhered material removing further material by ploughing of the opposing sliding surface. This process continued with losses due to ejection and also layer build-up from readhered material, until the resulting mechanically-mixed layers on both surfaces became work-hardened enough (Table 3) to resist and reduce wear. Lower losses were observed on extended sliding to 13,032 m at  $0.905 \text{ m.s}^{-1}$  [1].

#### 5.1.2 390 to 570°C

Between 390°C and 570°C, both oxide (formed from limited oxidation on metallic surfaces, evidenced by surface discolouration – Figs. 6 and 7) and metallic debris (produced by delamination wear – Figs. 11 and 12) were produced from both sample and counterface (Fig. 16, Region 2). This debris was not retained due to low residency and rapid ejection. The oxide debris was hence unable to compact and sinter, to form wear-protective compacted oxide layers.

Although wear-protective oxide layers could not form between 390 and 570°C, there was sufficient oxidation to severely reduce metallic adhesion. Thus readhesion of metallic debris to wear surfaces was more limited and patchier metallic transfer layers formed than seen at R.T. and 270°C. This was especially the case at  $0.314 \text{ m.s}^{-1}$  where greater retention of oxide (than at higher sliding speeds) restricted metallic debris readherence to a few isolated patches (Figs. 6 to 9). The absence of oxide ‘glaze’ layers and greatly reduced metallic transfer layers led to increased wear of both Incoloy MA956 and Incoloy 800HT unprotected surfaces (this enhanced wear continued up to

13,302 m [1]). Additionally, in the absence of such layers, reduced elevated temperature hardness of both Incoloy MA956 sample and Incoloy 800HT counterface surfaces probably facilitated easier removal of metallic material from both. Data collected by Rose [9] demonstrates reduced hardness with increasing temperature (Table 5).

Limited metallic debris was able to readhere to the Incoloy 800HT counterface within the wear track, forming the raised asperities seen at 570°C and above.

It was observed elsewhere [1] that a wear protective compacted Cr-Fe based oxide layer developed only when the sample was not in reciprocation (only the counterface was rotating) at 510°C (0.314 m.s<sup>-1</sup>). This demonstrates a significant degree of oxidation under these conditions and greater debris retention without reciprocation, which was responsible for promoting substantial debris ejection and prevention of oxide layer formation.

### 5.1.3 630 to 750°C

At 630°C, a further transition to ‘mild wear’ began to occur (Fig. 16, Region 3). The production of Incoloy MA956-sourced fine oxide debris (Fig. 11) increased sufficiently to outstrip losses by ejection. Such debris was able to build up and sinter to form potentially wear protective, high hardness ‘glaze’ layers (Table 6.4) on the Incoloy MA956 surface (Figs. 6 and 8). The extremely fine grain size (AFM [58] indicated as little as ~25 nm) suggests likely formation of a nano-structured ‘glaze’, seen elsewhere for the Nimonic 80A / Stellite 6 [1-4] and Incoloy MA956 / Stellite 6 [6] combinations. ‘Glaze’ also formed on the asperity tips within the Incoloy 800HT counterface wear track at 690 and 750°C (discussed in Section 5.2.2).

However, debris ejection was still sufficient to heavily retard oxide build-up and delay ‘glaze’ layer development (indicated by delayed reductions in frictional variability), allowing for an extended period of ‘severe wear’. This was especially so at higher sliding speed, which increased sliding temperature was needed to overcome. At 630°C, ‘glaze’ layer development was restricted to limited (0.654 m.s<sup>-1</sup>) or isolated (0.905 m.s<sup>-1</sup>) patches; this contrasted with clearer ‘glaze’ development at 0.314 m.s<sup>-1</sup>. At 690°C, oxide development increased such that more complete ‘glaze’ layers observed at 0.314 m.s<sup>-1</sup> also developed at 0.654 m.s<sup>-1</sup>, however, only patchy ‘glaze’ layers still formed at 0.905 m.s<sup>-1</sup>.

Only at 750°C and sliding speeds of 0.314 and 0.654 m.s<sup>-1</sup> was ‘glaze’ formation rapid enough to restrict metallic debris removal during early ‘severe wear’ and reduce sample wear, though damage was still not restricted to usable (i.e. minimal) levels. Decreases in frictional variability indicate reduced ‘metal-to-metal’ contact after ~1,036 m of sliding at 0.314 m.s<sup>-1</sup> and ~1,507 m at 0.654 m.s<sup>-1</sup>.

The still patchy ‘glaze’ formation at 0.905 m.s<sup>-1</sup>, even at 750°C, appears to have been too late to prevent increased wear (there was no reduction in frictional variability until after ~2,285 m). Also,

higher sliding speed subjected the 'glaze' layers to greater stress (as evidenced by increased 'glaze' fracture at  $0.905 \text{ m.s}^{-1}$ ), allowing more effective break-up and further inhibiting their development. After 4,522 m of sliding, only 40-50% 'glaze' layer coverage was achieved at  $0.905 \text{ m.s}^{-1} / 750^\circ\text{C}$  and extended sliding (up to 13,032 m) was required before comprehensive 'glaze' layers formed [1].

Further decreases in Incoloy MA956 and Incoloy 800HT strength between  $630^\circ\text{C}$  and  $750^\circ\text{C}$  allowed even greater removal of metallic (and developing oxide) material during the early 'severe wear' period. The continued production of large, flattened metallic debris (Figs. 11 and 12) indicated that prior to 'glaze' layer development, a delamination wear mechanism dominated.

#### 5.1.4 Categorisation of Observed Wear Modes

It was suggested previously that Quinn's 'mild' and 'severe' wear modes [59] could be sub-divided to better fit actual wear observations [7].

- 1) 'Severe wear' could be separated into '*standard severe wear*' (with adhesion and delamination producing a bright, torn metallic wear surface in the absence of oxide) and '*abrasion assisted severe wear*' (with oxide levels too low to prevent phenomena such as metallic contact, adhesion and delamination dominating, but sufficient to assist and enhance wear during sliding by abrasion, producing a smoother, more polished metallic wear surface).
- 2) Two forms of 'mild wear' were suggested. '*Protective mild wear*' was defined as either (a) loose oxide at low temperature or (b) 'glaze' layers at high temperature acting as a barrier to metallic contact and reducing wear. '*Abrasive mild wear*' was described as loose unsintered oxide preventing metallic contact but abrasively promoting high wear, denoted by very fine parallel grooves in the direction of sliding; at best the oxide only thinly smears the wear surface. 'Protective mild wear' was observed previously with high Co- [1-9] and Fe-Cr-based oxide [1, 6], both in low temperature loose oxide and elevated temperature 'glaze' layer forms. The poor sinterability of Ni-Cr-based oxide in low debris retention systems [1, 4, 5, 7] favoured 'abrasive mild wear' or 'abrasion assisted severe wear' at more elevated temperatures; previous literature showing this oxide to form 'glaze' have detailed higher debris retention systems [10, 20-24] and / or very high temperatures [46,60].

The wear seen between R.T. and  $270^\circ\text{C}$ , with a high degree of delamination and material transfer due to adhesion matches 'standard severe wear', with no oxide present to modify the wear process.

Between  $390^\circ\text{C}$  and  $570^\circ\text{C}$ , although limited oxide forms, inhibits adhesion and reduces transfer, metallic contact and delamination continues. The wear regime still fits in the 'standard severe wear' category, with the oxide showing no signs of significant abrasive (i.e. polishing) action or build-up into 'glaze'. This change in adhesion due to the oxide does imply 'high adhesion' and 'low adhesion' sub-categorisation is possible, though too much subdivision is potentially confusing.



The formation of potentially wear arresting ‘glaze’ layers (although not happening quickly enough at times to reduce wear) matches the ‘protective mild wear’ regime. There was no evidence of an ‘abrasive mild wear’ regime during the current study.

## 5.2 Cross-sectional Analysis

### 5.2.1 Sample Surface

The observed multi-layer structure of the debris at 750°C and sliding speeds of 0.314 and 0.905 m.s<sup>-1</sup> (Figs. 14 and 15) indicates various stages of debris development, leading to generation of fine oxide capable of forming ‘glaze’ (Fig. 17):

- 1) metallic debris removal and redeposition of this debris back onto the Incoloy MA956 sample during the early stages of wear, forming a deformed, limited metallic debris layer overlying undamaged Incoloy MA956 base metal;
- 2) progressive debris break-down and oxidation with increased sliding, this debris being deposited to form an exclusively Incoloy MA956-sourced mixed metal-oxide layer – oxide levels in the debris increased with further sliding;
- 3) at 0.905 m.s<sup>-1</sup> only, oxide levels increased until the debris was completely oxidized – this formed an entirely oxidised sub-layer overlying the mixed metal-oxide debris layer;
- 4) later generation of an Incoloy MA956-sourced Cr<sub>1.3</sub>Fe<sub>0.7</sub>O<sub>3</sub> phase fine debris, due to on-going debris break-down from continued sliding contact between the mixed metal-oxide debris layer (or completely oxidised sub-layer at 0.905 m.s<sup>-1</sup>) and the Incoloy 800HT counterface; and
- 5) sintering and compaction of this fine oxide debris into hard, wear protective, nano-structured ‘glaze’ layers, overlying the earlier developed debris layers on the Incoloy MA956 surface and causing the onset of mild wear – the ‘glaze’ is subject to continual break-down and reformation.

It was difficult at times to distinguish between the ‘glaze’ layer and the underlying debris, as is clear from the Figs. 14 and 15 cross-sections. However, an absence of coarser debris (>3 µm) within the top ~2 µm of the debris surface enabled differentiation of ‘glaze’ under such circumstances.

At 750°C, both the earlier metallic debris and the later oxide debris were Fe-Cr based; the material making up the layers was removed from and redeposited back onto the Incoloy MA956. There was negligible intermixing of Incoloy 800HT-sourced counterface material (with only 0 to 3% counterface-sourced Ni). Apart from the dominance of sample-sourced material, the described sequence of events is similar to that suggested for Nimonic 80A versus Stellite 6 [2, 4].

The higher than expected Al in the ‘glaze’ layers (Figs. 14 and 15 – 0.314 and 0.905 m.s<sup>-1</sup> at 750°C) was due to Al diffusion to ‘glaze’ layer surfaces, where it underwent preferential oxidation (also observed for Incoloy MA956 versus Stellite 6 at 0.905 m.s<sup>-1</sup> and 750°C [1,6]). At 0.314 m.s<sup>-1</sup>,

surface Al content reached ~12%, and in isolated areas as high as ~24%; at 0.905 m.s<sup>-1</sup>, levels of 15 to 20% were achieved with some readings up to ~32%. The source of this Al was the mixed Incoloy MA956-sourced metal-oxide debris layers (and / or the wholly oxidised sub-layer at 0.905 m.s<sup>-1</sup>) underlying the ‘glaze’ and possibly the undeformed Incoloy MA956 itself. The effect of this Al on ‘glaze’ layer formation and properties is currently unclear, however, Al elsewhere has readily formed ‘glaze’ [30].

A non-uniform distribution of elements was observed elsewhere by Wood et al. [61], where Co and Mo diffused to the ‘glaze’ surface during ‘like-on-like’ sliding of Tribaloy 400C (‘rotating collar’ versus ‘fixed disc’, 600°C, sliding speed 3 m.s<sup>-1</sup>). An initial layer of Cr<sub>2</sub>O<sub>3</sub> (formed by removal and redeposition of transient oxidation) was replaced as sliding proceeded, by discrete layers of mainly Co-based oxide overlying mainly Mo-based oxide, then a mixed layer of Co, Cr, Mo and Si-based oxides after 3 hours of sliding. Such layers formed despite the 3 m.s<sup>-1</sup> sliding speed creating a high mixing potential at the wear interface; this may be related to high debris retention and stable ‘glaze’ formation allowing time for such diffusion effects to appear. This contrasts with earlier literature suggesting a more homogeneous oxide layer [10]. Further break-down and mixing on extended sliding to 12 hours, however, led to a more even distribution of elements [61].

### 5.2.2 Counterface Surface

The order of events on the Incoloy 800HT counterface is less clear as cross-sectional analysis was not possible due to extensive damage and difficulties in counterface sectioning. However, a likely order of events is as follows:

- 1) The Incoloy 800HT counterface at ‘glaze’ forming temperatures (630°C to 750°C) underwent ‘severe wear’ (via delamination) early in the sliding process, leading to the formation of the 1.5 mm deep wear track;
- 2) Some metallic debris was deposited onto the wear track to form asperities, as evidenced by many of the asperities rising ~1.5 mm above the original level of the unworn counterface surface (Fig. 6).
- 3) Subsequent ‘glaze’ development was restricted to the tips of these asperities (Fig. 13b), where they were in contact with and able to remove material from the Incoloy MA956 sample surface. At 750°C, this intermediate composition ‘glaze’ (~18% Ni, ~20% Cr, ~58% Fe at 0.314 m.s<sup>-1</sup>; ~16% Ni, ~21% Cr, ~58% Fe at 0.905 m.s<sup>-1</sup>) formed due to transfer and mixing of probably already oxidised Incoloy MA956-sourced material with Incoloy 800HT-based material.

At the same stage, some Incoloy MA956-sourced material collected in the bottom of the counterface wear scar as loose oxide debris, instead of being ejected.

Wear scar morphology at 690°C was near-identical to that at 750°C, suggesting ‘glaze’ on the asperity tips was similarly generated at this lower temperature.

The source material of the metallic asperities formed within the Incoloy 800HT counterface wear track on which the ‘glaze’ formed is also unclear – the mixed composition of the ‘glaze’ suggests they were either readhered Incoloy 800HT and / or a mixed Incoloy 800HT / Incoloy MA956 (sample) composition.

### 5.3 Microstructure and Second Phases

At 690 and 750°C, thermally induced material softening and plastic deformation (i.e. creep) of the Incoloy MA956 samples also needs consideration. Additionally, shear and frictional heating at the wear interface (especially at 0.905 m.s<sup>-1</sup>) may increase the number of operational slip planes [51, 52] and further assist deformation; this may reduce bulk material support for ‘glaze’ layers notably at higher sliding speed. However, it is unclear whether deformation would occur only during early ‘severe wear’ or also continue after ‘glaze’ formation (i.e. material ‘creep’ under the ‘glaze’ layer; also enhanced heating would retard any work-hardening effects resulting from sliding-induced deformation).

The high number of slip planes available in ‘body-centred cubic’ (Incoloy MA956) and ‘face-centred cubic’ (Incoloy 800HT) materials appear to be allowing deformation mechanisms to operate more deeply into the surface encouraging greater removal (i.e. allowing the much observed delamination mechanism). During the current study, cumulative damage on the counterface led to material of up to 1.5 mm depth being removed.

Also, continued deformation and ready material removal (at least during ‘severe wear’) suggests both materials’ second phases (meant to improve bulk mechanical properties) have not improved either alloys’ wear resistance, at least to a useful level. This may be due to the second phases’ relatively low density in both materials; dislocation movement and slip plane operation may not be impeded sufficiently to resist the high, localized shear stresses near the sliding surface. Moreover, these second phase particles can assist delamination wear due to dislocation pile-up and coalescence to form sub-surface voids [62] (a comparative study – with varying levels of second phases and also without them – is suggested to investigate their actual effect).

Such deformation was absent when Incoloy MA956 was slid against a Stellite 6 counterface [6], where more rapid ‘glaze’ formation apparently better protected the Incoloy MA956 surface; this appears partially attributable to Co-transfer from the Stellite 6 [6]. Also, the presence of a ‘hexagonal-close-packed’ phase restricting material removal to Stellite 6’s extreme surface, may have reduced or impeded material transfer and back-transfer evident with the ‘Incoloy MA956 versus Incoloy 800HT’ wear pair. The fewer slip planes and the shear-induced alignment of the operational basal plane within ‘hexagonal-close-packed’ phases is, as described earlier, restricting wear to the extreme surface [48,49].

The high wear and deformation of especially the Incoloy MA956 at elevated temperature has shown that lack of base metal mechanical support does not necessarily prevent 'glaze' formation. However, such support is necessary if a 'glaze' is to provide effective wear protection within a sliding system, in that a stable base allows sustainment of 'glaze' layers without creep / deformation undermining them. Additionally, the base material must not undergo excessive wear before comprehensive 'glaze' layers form, as their wear protection function is rendered effectively redundant if the material to be protected is already heavily damaged.

The current and recent [1,5-7] observations bear some similarities to those in Crook and Li's comparative 'like-on-like' studies on Stellite 6, Stellite 1 (higher C, Cr and W than Stellite 6), Stellite 2006 (an Fe-Cr-33% Co alloy), Haynes No. 716 (an Ni-Fe-Cr alloy with 11% Co) and Haynes No. 6 (an Ni-Cr alloy with no Co), indicating generally better metal-to-metal wear with increasing levels of Co up to 750°C [46]. This superior wear resistance was attributed to the previously discussed better galling resistance and 'face-centred cubic' to 'hexagonal-close-packed' transformation seen in some Co-based alloys. Only at higher temperature (~1,000°C) did all these alloys exhibit low wear with protective oxide layer formation, though there was no discussion of thermally induced metallic substrate softening, deformation and loss of underlying support. However, Crook and Li used a 'button-on-disc' system, thus it is uncertain whether softening and deformation effects would be as readily observed as with the current 'block-on-cylinder' system.

## **6. Summary of Results**

Similar observations were made regardless of sliding speed, with three distinct regions of behaviour largely dependent on temperature.

- 1) At R.T. and 270°C, an absence of oxide debris allowed direct contact between the Incoloy MA956 sample and Incoloy 800HT counterface. 'Severe wear' by delamination produced large metallic debris sourced from both, some of which readhered forming a work-hardened, mechanically mixed metallic transfer layer that limited wear. The layer's heterogeneous composition indicated incomplete mixing.
- 2) Between 390°C and 570°C, both oxide and metallic debris were produced from both sample and counterface. Although the oxide debris did not form wear protective layers, it reduced metallic debris readhesion and formation of a metallic transfer layer. Both the oxide and metallic debris were instead ejected. Reductions in hardness of both metals with temperature may also have facilitated easier material removal. Wear of both sample and counterface was thus increased.
- 3) At 630°C and 690°C, a further transition to 'mild wear' occurred due to increased production of Incoloy MA956-sourced oxide debris outstripping that lost by ejection; this debris could thus build up into wear-protective, nano-structured 'glaze' layers. Enhanced debris ejection still retarded oxide build-up and there was still an extended period of 'severe wear' during early

sliding. Wear levels during this initial ‘severe wear’ phase were sufficient to continue the trend of increased wear with temperature.

Only at 750°C (0.314 and 0.654 m.s<sup>-1</sup>) was oxidation and ‘glaze’ formation rapid enough to restrict early ‘severe wear’ and reduce overall wear.

Increasing sliding speed had some subtle influences, largely due to enhanced ejection. Firstly, the appearance of oxide between 390°C and 570°C was less able to retard metallic transfer at 0.654 and 0.905 m.s<sup>-1</sup>, hence patchy Incoloy MA956 metallic transfer layers did form. Secondly, ‘glaze’ layer formation was retarded by enhanced sliding speed, which higher temperatures were required to overcome. Finally, retarded ‘glaze’ development at 0.905 m.s<sup>-1</sup> and 750°C failed to halt increased wear; as well as by debris ejection, ‘glaze’ layer development was inhibited by increased fracture and break-up.

Autopoint EDX indicated the formation of a multi-layered structure on the Incoloy MA956 surface on sliding at 750°C (Figs. 14 and 15), composed of:

- 1) a deformed, limited metallic debris layer formed during the early stages of wear, by removal of metallic debris from and redeposition of this debris back onto the Incoloy MA956 sample;
  - 2) an exclusively Incoloy MA956-sourced mixed metal-oxide layer, which developed by progressively greater oxidation of Incoloy MA956-sourced metallic debris with increased sliding;
  - 3) at 0.905 m.s<sup>-1</sup>, a wholly oxidised sub-layer also formed overlying the mixed metal-oxide layer;
  - 4) later generation of fine Incoloy MA956-sourced debris, due to on-going debris break-down from continued sliding contact between the mixed metal-oxide debris layer (or wholly oxidised sub-layer at 0.905 m.s<sup>-1</sup>) and the Incoloy 800HT counterface; and
  - 5) a wear-protective, nano-structured oxide ‘glaze’ layer develops due to sintering and compaction of this fine oxide debris, overlying the earlier developed debris layers on the Incoloy MA956 and leading to mild wear – the ‘glaze’ is subject to continued break-down and reformation.
- 6) The ‘glaze’ layers also contained elevated Al concentrations, due to diffusion and preferential oxidation of Al from within the debris layer and possibly the underlying Incoloy MA956 sample material. Al influence on ‘glaze’ formation and properties is, however, unclear.

Wear of the Incoloy 800HT counterface showed the following patterns:

- 1) Up to 570°C, counterface wear mirrored Incoloy MA956 sample wear, with metallic transfer layers forming at R.T. and 270°C, and increased damage accompanying reduced metallic transfer (due to increasing oxidation inhibiting adhesion) at 390, 450 and 510°C.
- 2) Between 570°C and 750°C the counterface continued to undergo ‘severe wear’, during which limited metallic debris adhesion to the wear track formed asperities (Fig. 6).

- 3) The asperity formation was followed at 750°C (and probably 690°C) by ‘glaze’ development on the asperity tips, due to mixing of Incoloy MA956 sample and Incoloy 800HT counterface-sourced material. Whether the metallic asperities were redeposited Incoloy 800HT or were of a mixed Incoloy MA956 / Incoloy 800HT composition is, however, uncertain.

Although ‘glaze’ formation did reduce wear at high temperature, this was not to acceptable levels due to continuing early ‘severe wear’. Also, it is possible that material softening and deformation reduced bulk material support for the ‘glaze’. There is additionally nothing to suggest that either the Incoloy MA956 or Incoloy 800HT second phases, meant to improve bulk mechanical properties, improved wear resistance to a useful level.

### **Acknowledgements**

Grateful acknowledgements are made to the UK Engineering Physics Science Research Council (EPSRC) and British Gas for their financial backing, and also to Northumbria University for their day-to-day support of this project.

### **References**

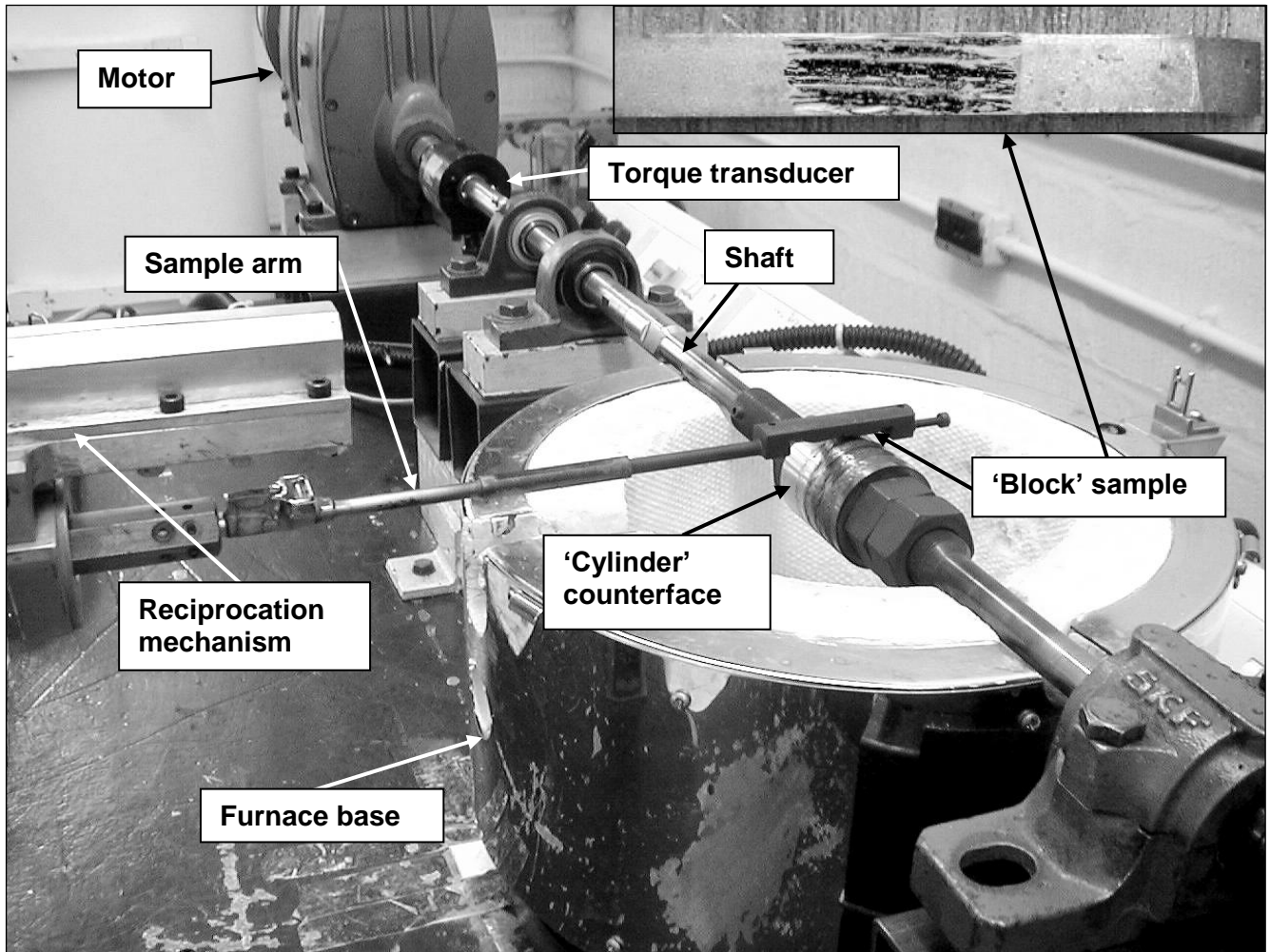
- [1] I.A. Inman, Ph.D. Thesis “Compacted Oxide Layer Formation under Conditions of Limited Debris Retention at the Wear Interface during High Temperature Sliding Wear of Superalloys”, Northumbria University, UK (2003), published by [‘Dissertation.com’](http://Dissertation.com) (2006).
- [2] I.A. Inman, S. Datta, H.L. Du, J.S. Burnell-Gray, S. Pierzgalski, Q. Luo “Microscopy of ‘glazed’ layers formed during high temperature sliding wear at 750°C”, *Wear* 254 (2003) 461-467.
- [3] S. Datta, I. Inman, H.L. Du, Q. Luo “Microscopy of ‘glazed’ layers formed during high temperature wear, Invited Talk at the Institute of Materials”, Tribology Meeting, London, November 2001.
- [4] I.A. Inman, S. Datta, H.L. Du, J.S. Burnell-Gray, S. Pierzgalski and Q. Luo “Studies of High Temperature Sliding Wear of Metallic Dissimilar Interfaces”, *Tribology International* 38 (2005) 812–823.
- [5] I.A. Inman, S.R. Rose, P.K. Datta “Development of a Simple ‘Temperature versus Sliding Speed’ Wear Map for the Sliding Wear Behaviour of Dissimilar Metallic Interfaces”, *Wear* 260 (2006) 919–932.
- [6] I.A. Inman, S.R. Rose, P.K. Datta “Studies of High Temperature Sliding Wear of Metallic Dissimilar Interfaces II: Incoloy MA956 versus Stellite 6”, *Tribology International* 39 (2006) 1361–1375.
- [7] I.A. Inman, P.S. Datta “Development of a Simple ‘Temperature versus Sliding Speed’ Wear Map for the Sliding Wear Behaviour of Dissimilar Metallic Interfaces II” *Wear* 265 (2008) 1592–1605.

- [8] P.D. Wood, Ph.D. Thesis “The Effect of the Counterface on the Wear Resistance of Certain Alloys at Room Temperature and 750°C”, Northumbria University, UK (1997).
- [9] S.R. Rose, Ph.D. Thesis “Studies of the High Temperature Tribological Behaviour of Some Superalloys”, Northumbria University, UK (2000).
- [10] F.H. Stott, D.S. Lin, G.C. Wood “The structure and mechanism of formation of the “glaze” oxide layers produced on Ni-based alloys during wear at high temperatures”, *Corrosion Science* 13 (1973) 449 - 469.
- [11] M. Johnson, P. Moorhouse, J.R. Nicholls, DTI Industry Valve Project, 61-68 (1990).
- [12] J-N. Aoh, J-C. Chen “On the wear characteristics of Co-based hardfacing layer after thermal fatigue and oxidation”, *Wear* 250-251 (2001) 611.
- [13] Singh, J. and Alpas, A.T. “High-temperature Wear and Deformation Processes in Metal Matrix Composites,” *Metallurgical and Materials Transactions A*, 27 (1996) 3135-3148.
- [14] F.H. Stott, J. Glascott, G.C. Wood “Factors affecting the progressive development of wear-protective oxides on Fe-base alloys during sliding at elevated temperatures”, *Wear* 97 (1984) 93-106.
- [15] M.G. Gee, N.M. Jennett “High resolution characterisation of tribochemical films on alumina”, *Wear* 193 (1995) 133-145.
- [16] P.D. Wood, P.K. Datta, J.S. Burnell-Gray, N. Wood “Investigation into the high temperature wear properties of alloys contacting against different counterfaces, Materials Science Forum”, 251-254 (1997) 467-474.
- [17] Wisbey, C.M. Ward-Close, *Materials Science and Technology* “Wear resistant surfaces on high temperature titanium alloy and titanium aluminide by diffusion bonding”, 13 (1997) 349-355.
- [18] J. Jiang, F.H. Stott, M.M. Stack, ”The effect of partial pressure of O on the tribological behaviour of a Ni-based alloy, N80A, at elevated temperatures”, *Wear* 203-204 (1997) 615-625.
- [19] X.Y. Li, K.N. Tandon “Microstructural characterization of mechanically mixed layer and wear debris in sliding wear of an Al alloy and an Al based composite”, *Wear* 245 (2000) 148-161.
- [20] J. Jiang, F. H. Stott, M. M. Stack “A generic model for dry sliding wear of metals at elevated temperatures” *Wear* 256 (2004) 973-985.
- [21] J. Jiang, F. H. Stott, M. M. Stack “The role of tribo-particulates in dry sliding wear” *Trib. Int.* 31-5 (1998) 245-256.
- [22] J. Jiang, F. H. Stott, M. M. Stack “Characterization of wear scar surfaces using combined three-dimensional topographic analysis and contact resistance measurements” *Trib. Int.* 30-7 (1997) 517-526.
- [23] J. Jiang, F. H. Stott, M. M. Stack “A mathematical model for sliding wear of metals at elevated temperatures” *Wear* 181-183 (1995) 20-31.
- [24] J. Jiang, F. H. Stott, M. M. Stack “Some frictional features associated with the sliding wear of the Ni-base alloy N80A at temperatures to 250°C” *Wear* 176 (1994) 185-194.

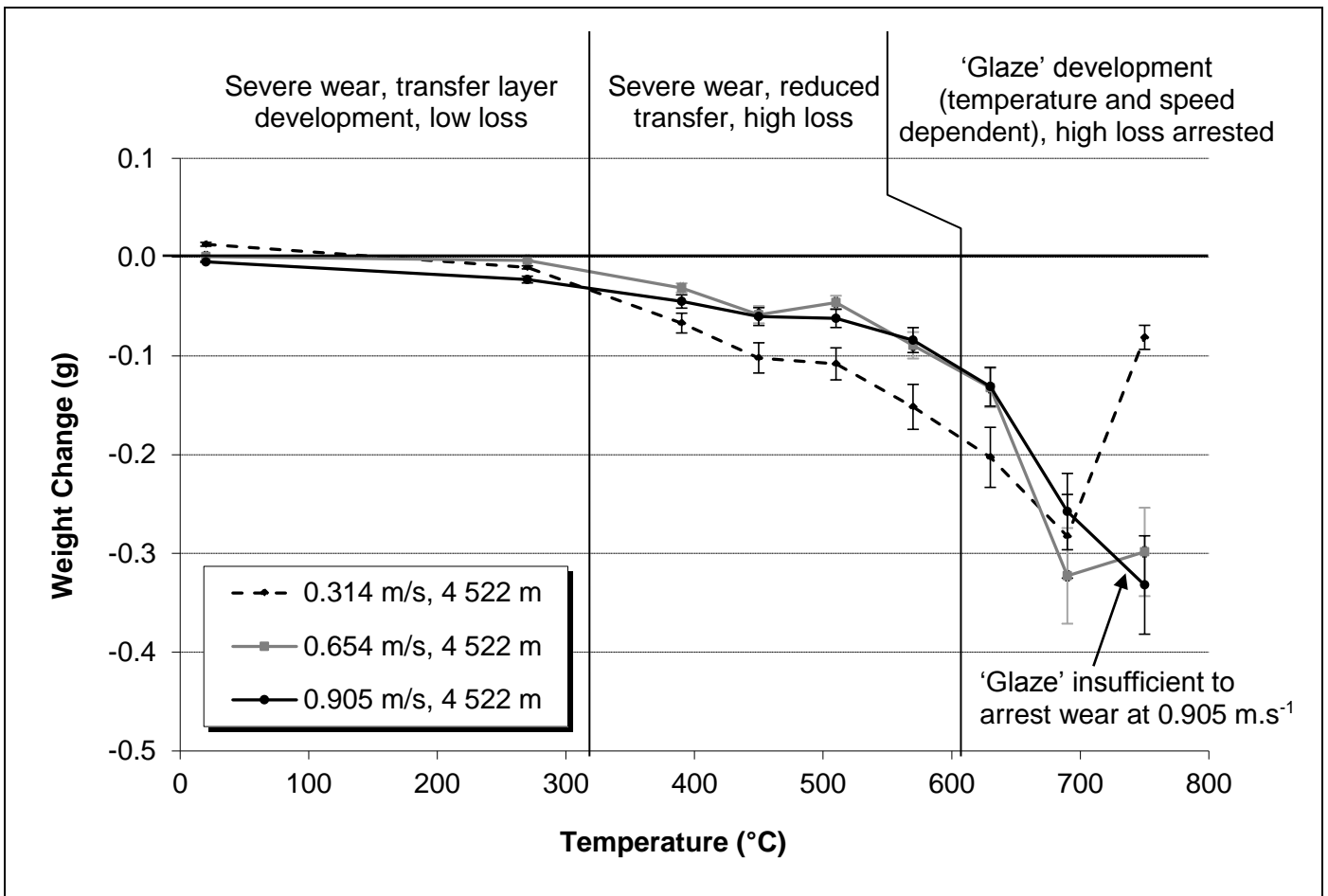
- [25] J.K. Lancaster "The Formation of Surface Films at the Transition Between Mild and Severe Metallic Wear", Proc. Royal Society London, A 273 (1962) 466-483.
- [26] N.C. Welsh "The Dry Wear of Steels 1, the General Pattern of Behaviour" Phil. Trans., 257A (1965) 31-50.
- [27] N.C. Welsh "The Dry Wear of Steels 2, Interpretation and Special Features" Phil. Trans., 257A (1965) 51-70.
- [28] H. So "Characteristics of Wear Results Tested by Pin-on-Disc at Moderate to High Speeds", Tribol. Int., Vol. 25, No. 5 (1996) 415-423.
- [29] H. So "Wear Behaviours of Laser-Clad Stellite Alloy 6", Wear 192 (1996) 78-84.
- [30] C. Subramaniam "Wear of Al-12.3 Wt% Si Alloy Slid Against Various Counterface Materials" Scripta Metallurgica 25 (1991) 1369-1374.
- [31] P.J. Blau "Mechanisms for Traditional Friction and Wear Behaviour of Sliding Metals" Wear 72 (1981) 55-66.
- [32] P.D. Wood, H.E. Evans, C.B. Ponton "Investigation into The Wear Films Formed on Certain Superalloys between 20 and 600°C during Rotation in an Unlubricated Bearing" Proc. ASME/STLE Int. Joint Tribol. Conf. 2009 (Oct. 19-21, 2009) Memphis, Tennessee, USA.
- [33] S.C. Lim "Recent Development in Wear Maps", Tribol. Int. 31, Nos. 1-3 (1998) 87-97.
- [34] S.C. Lim "The relevance of wear-mechanism maps to mild-oxidational wear", Tribol. Int. 35, No. 11 (2002) 717-723.
- [35] T.H.C. Childs "The Sliding Wear Mechanisms of Metals, Mainly Steels", Tribol. Int. 13 (1980) 285-293.
- [36] A. R. Riahi and A. T. Alpas – "Wear map for grey cast Fe" Wear 255 (2003) 401-409.
- [37] H. Chen and A. T. Alpas – "Sliding wear map for the magnesium alloy Mg-9Al-0.9 Zn (AZ91)" Wear 246 (2000) 106-116.
- [38] S.H. Yang, H. Kong, E-S. Yoon and D.E. Kim – "A wear map of bearing steel lubricated by silver films" Wear 255 (2003) 883-892.
- [39] D. Grimanelisa and T.S. Eyre "Wear characteristics of a diffusion bonded sintered steel with short term surface treatments" Wear 262 (2007) 93-103.
- [40] D. Grimanelisa and T.S. Eyre – "Sliding wear mapping of an ion nitrocarburized low alloy sintered steel" Surf. & Coat. Tech. 201-6 (2006) 3260-3268.
- [41] K. Elleuch, R. Elleuch, R. Mnif, V. Fridrici and P. Kapsa – "Sliding wear transition for the CW614 brass alloy" Tribol. Int. 39-4 (2006) 290-296.
- [42] S. Anbuselvan and S. Ramanathan – "Dry sliding wear behavior of as-cast ZE41A magnesium alloy" Materials & Design 31-4 (2010) 1930-1936.
- [43] T. Gómez-del Río, A. Rico, M.A. Garrido, P. Poza and J. Rodríguez – "Temperature and velocity transitions in dry sliding wear of Al-Li/SiC composites" Wear 268, Issues 5-6 (2010) 700-707.
- [44] K. Kato and K. Hokkirigawa "Abrasive Wear Diagram", Proc. Eurotrib '85, Vol. 4, Section 5.3, Elsevier, Amsterdam (1985) 1-5.



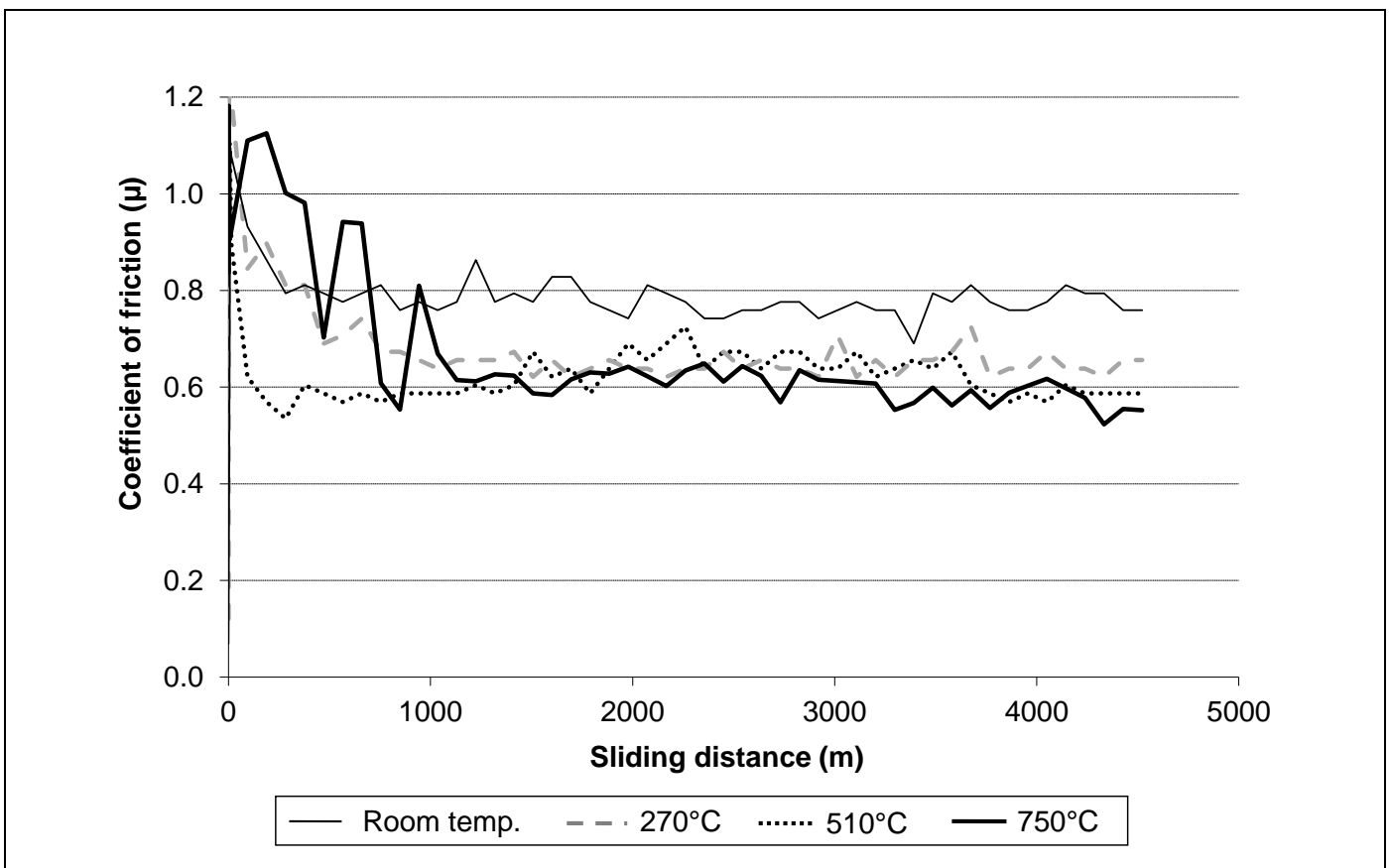
- [45] K. Adachi, K. Kato and N. Chen "Wear map of ceramics" *Wear* 203-204 (1997) 291-301.
- [46] P. Crook and C.C. Li "The Elevated Temperature Metal-to-Metal Wear Behaviour of Selected Hard Facing Alloys" *Wear of Materials*, ASME Publication 110254, (1983) 272-279.
- [47] D.H.E. Persson "Laser processed low friction surfaces", Licentiate of Philosophy Dissertation, Uppsala University (2003).
- [48] D.H.E. Persson "On the Mechanisms behind the Tribological Performance of Stellites", Ph.D. Thesis, Uppsala University (2003).
- [49] D.H. Buckley "Adhesion, Friction and Wear of Cobalt and Cobalt-Base Alloys" *Cobalt* 38 (1968) 20-28.
- [50] F.H. Stott, C.W. Stevenson and G.C. Wood – "Friction and Wear Properties of Stellite 31 at Temperatures from 293 to 1074K" *Metals Tech.*, 4 (1977) 66-74.
- [51] V. John "Introduction to engineering materials" Industrial Press (1992).
- [52] G.T. Murray "Introduction to engineering materials: behaviour, properties, and selection" Marcel Dekker (1993).
- [53] D.A. Rigney and W.A. Glaeser "The Significance of Near Surface Microstructure in the Wear Process" *Wear* 46 (1978) 241-250.
- [54] M. Sawa and D.A. Rigney "Sliding Behaviour of Dual Phase Steels in Vacuum and in Air", *Wear* 119 (1987) 369-390.
- [55] P. Heilmann, J. Don, T.C. Sun, D.A. Rigney, W.A. Glaeser "Sliding Wear and Transfer", *Wear* 91 (1983) 171-190.
- [56] M. Bartsch, A. Wasilkowska, A. Czyrska-Filemonowicz and U. Messerschmidt "Dislocation Dynamics in the Oxide Dispersion Strengthened Alloy Incoloy MA956", *Mat. Sci. Eng.*, A272 (1999) 152-162.
- [57] Private Communication, Special Metals (Wiggins) Ltd.
- [58] I.A. Inman, P.S. Datta, H.L. Du, C. Kübel, P.D. Wood "High Temperature Tribocorrosion", in: T. Richardson, B. Cottis, R. Lindsay, S. Lyon, D. Scantlebury, H. Stott and M. Graham (Eds.), *Shreir's Corrosion – VOL 1: Types of High Temperature Corrosion*, Elsevier Ltd. (2009)
- [59] T.F.J. Quinn "Review of Oxidational Wear. Part 1: The Origins of Oxidational Wear" *Tribo. Int.*, 16 (1983) 257-270.
- [60] J.Yoshihisa, F.Yokoyama, T.Yamasaki, N.Ohmae, "The Tribological Characteristics of Ni-Cr Cast Alloy at 1000 Degree C in Air", *Tribology Online*, Vol. 5, No. 1, (2010) 27-32.
- [61] P.D.Wood, H.E.Evans, C.B.Ponton "Investigation into the Wear Behavior of Tribaloy 400C during Rotation as an Unlubricated Bearing at 600°C from 2 Minutes to 12 Hours", to be published in *Wear*.
- [62] N.P. Suh "The Delamination Theory of Wear" *Wear* 25 (1973) 111-124.



**Fig. 1:** Reciprocating high temperature block-on-cylinder wear rig plus an Incoloy MA956 'block' sample (shown example with 'glaze' layer formed by sliding at  $0.314 \text{ m.s}^{-1}$  and  $750^\circ\text{C}$  against an Incoloy 800HT 'cylinder' counterface – load 7N, sliding distance 4,522 m)



**Fig. 2:** Effect of temperature on weight change – Incoloy MA956 vs. Incoloy 800HT (load = 7N, sample size = 3)





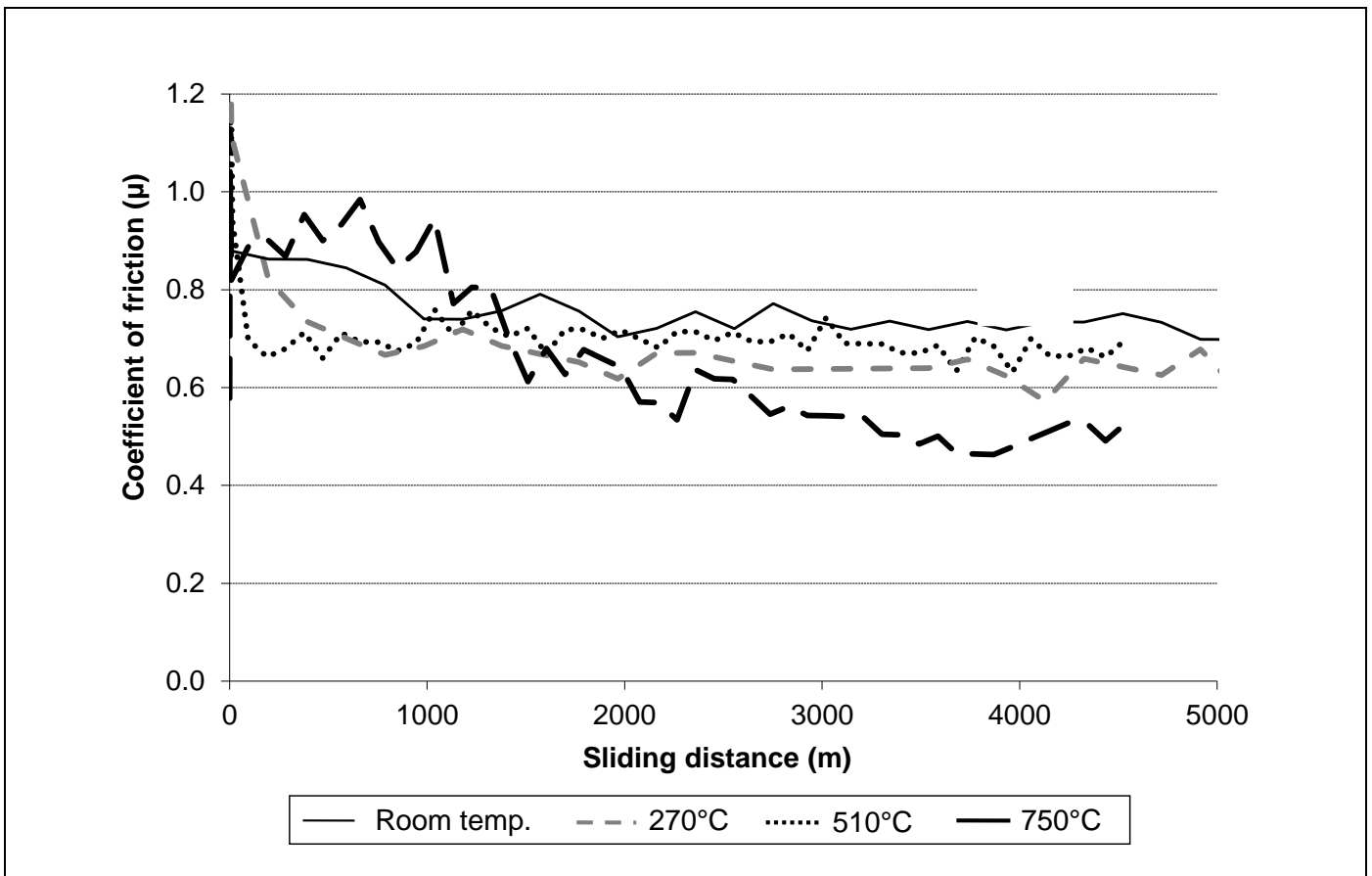



**Fig. 3:** Effect of temperature on friction at 0.314 m.s<sup>-1</sup> – Incoloy MA956 vs. Incoloy 800HT (load = 7N, sample size = 3)

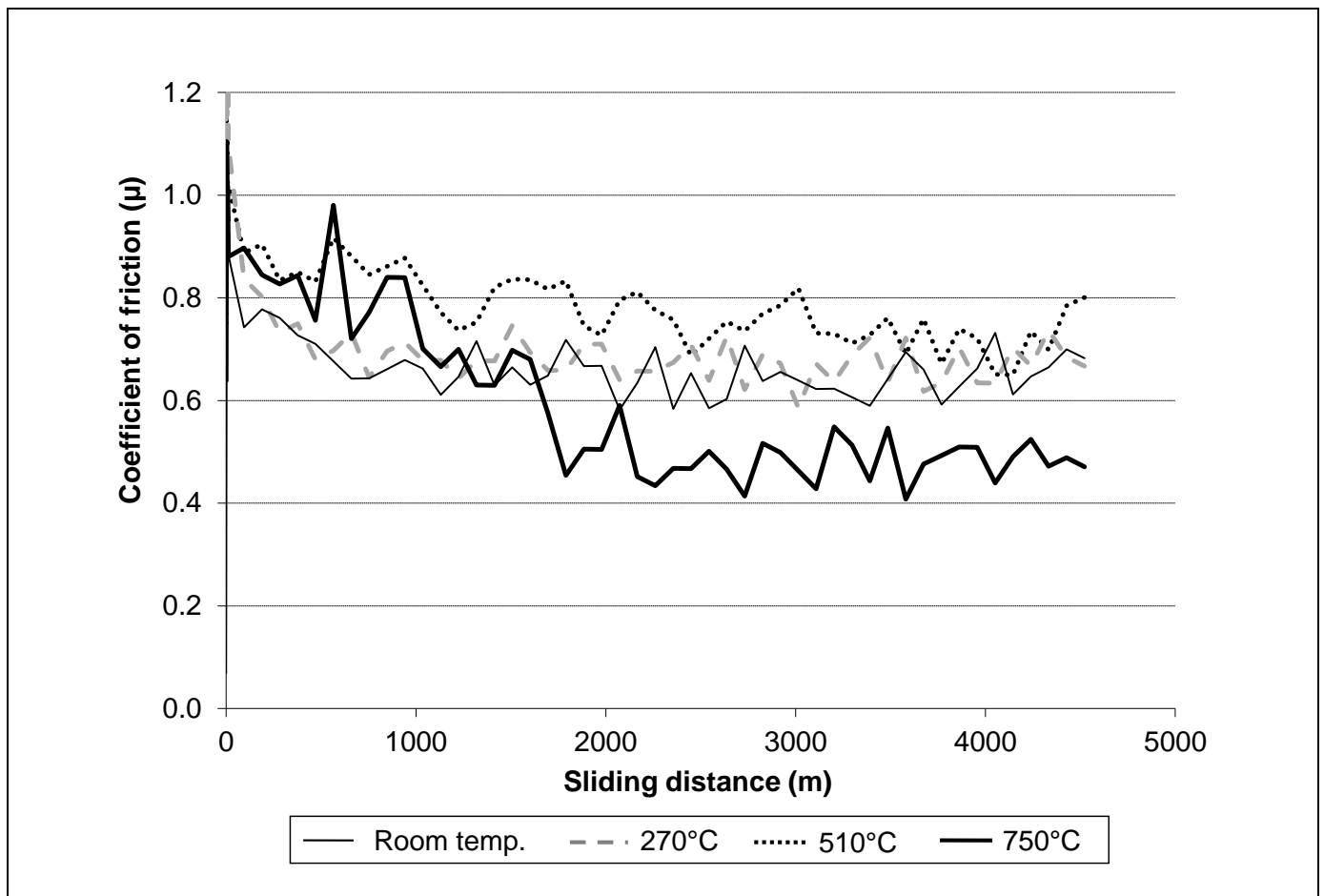






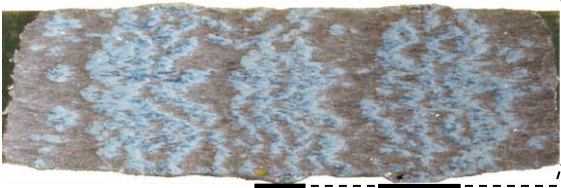
**Fig. 4:** Effect of temperature on friction at  $0.654 \text{ m.s}^{-1}$  – Incoloy MA956 vs. Incoloy 800HT (load = 7N, sample size = 3)



**Fig. 5:** Effect of temperature on friction at  $0.905 \text{ m.s}^{-1}$  – Incoloy MA956 vs. Incoloy 800HT (load = 7N, sample size = 3)

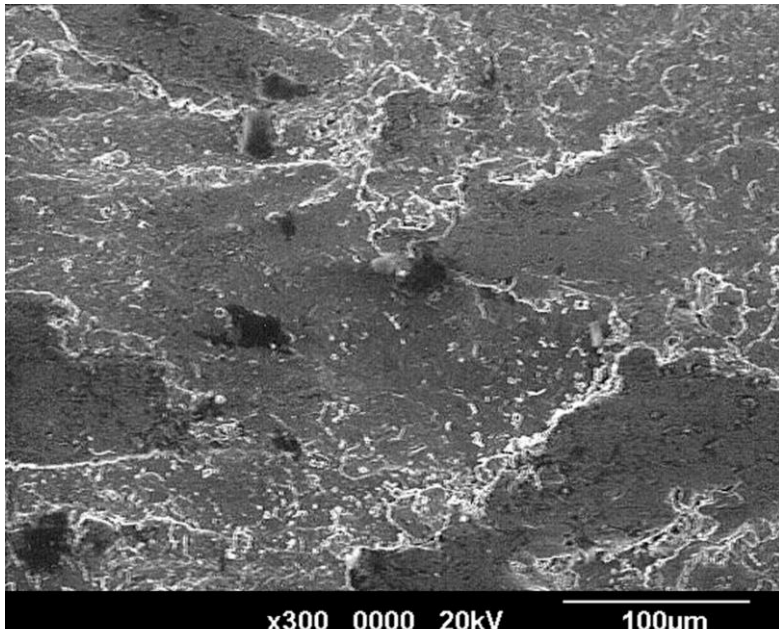
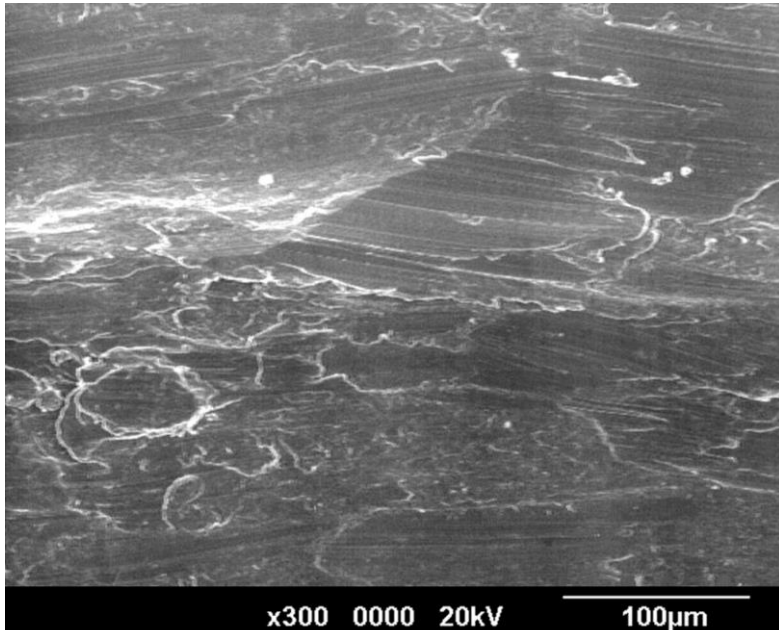
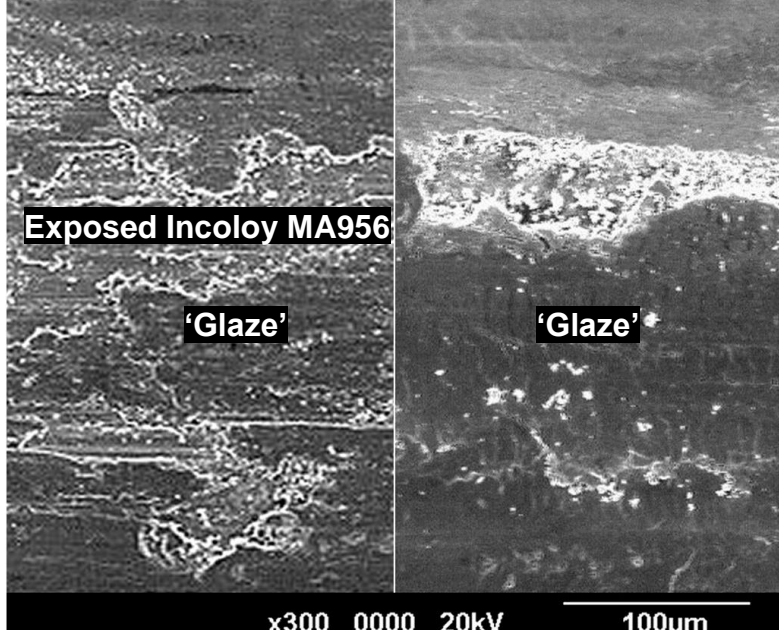
	<p><b>Room Temperature, 4,522 m – sample</b>  <i>(wear scar = 15 x 5 mm)</i>  Transfer layer covering 90% of wear scar</p>
	<p><b>270°C, 4,522 m – sample</b>  <i>(wear scar = 17 x 5 mm)</i>  Transfer layer covering 80% of wear scar</p>
	<p><b>510°C, 4,522 m – sample</b>  <i>(wear scar = 18 x 5 mm, also 390, 450, 570°C)</i>  Reduced transfer (10%), now in more isolated patches –  discoloration due to limited oxidation of wear surface</p>
	<p><b>630°C, 4,522 m – sample</b>  <i>(wear scar = 20 x 5 mm)</i>  'glaze' covering large areas of highly worn wear scar, with  no evidence of metallic transfer</p>
	<p><b>750°C, 4,522 m – sample</b>  <i>(wear scar = 19 x 5 mm, also 690°C)</i>  'glaze' covering most of wear scar, no evidence of metallic  transfer</p>

**Fig. 6:** Optical Images for Incoloy MA956 versus Incoloy 800HT at 0.314 m.s<sup>-1</sup>

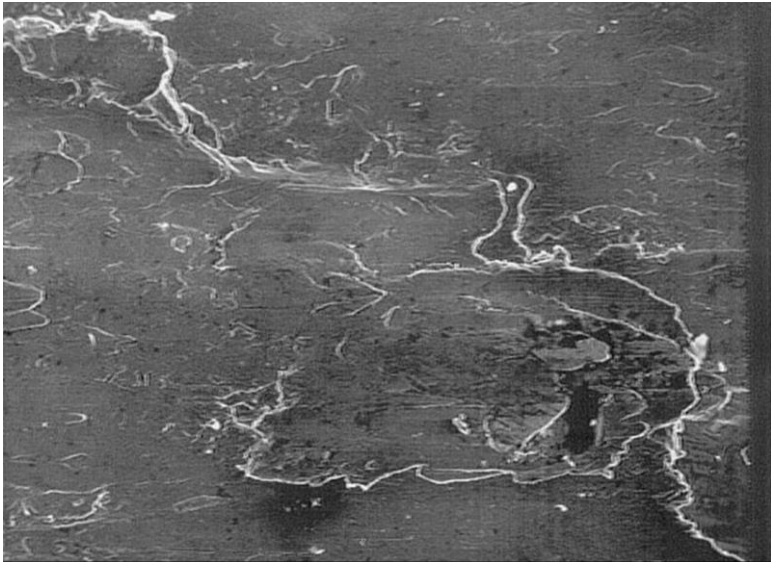
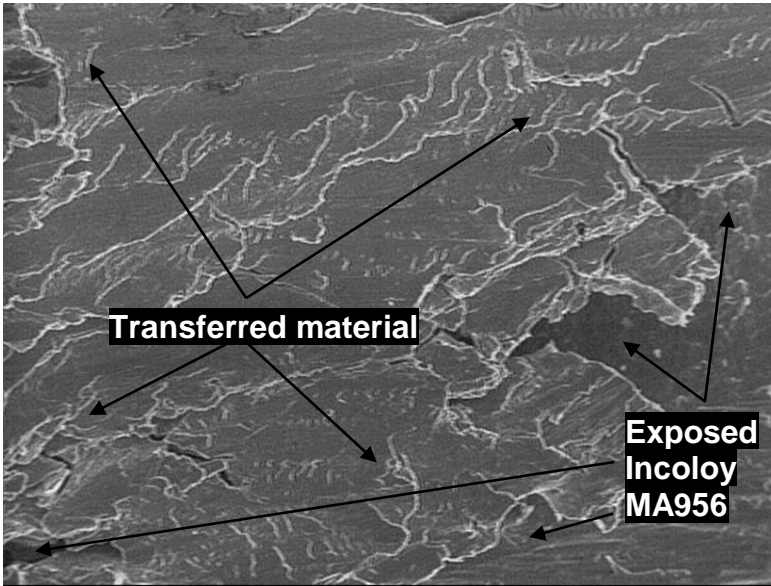
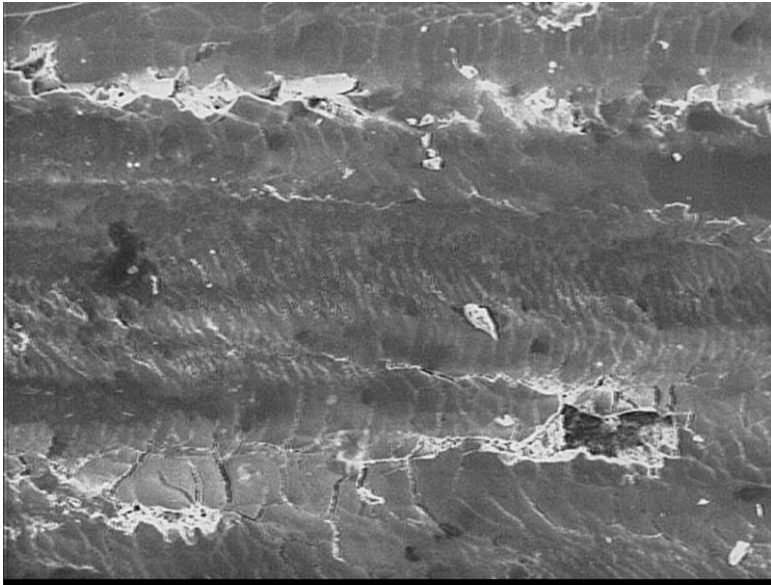
	<p><b>Room Temperature, 4,522 m – sample</b>  <i>(wear scar = 15 x 5 mm)</i>  Transfer layer covering 90% of wear scar</p>
	<p><b>270°C, 4,522 m – sample</b>  <i>(wear scar = 15 x 5 mm)</i>  Transfer layer covering 75% of wear scar</p>
	<p><b>510°C, 4,522 m – sample</b>  <i>(wear scar = 18 x 5 mm, also 390, 450, 570°C)</i>  Reduced metallic transfer with incomplete transfer layers (50%), though greater than at 0.314 m.s<sup>-1</sup> – increasing discoloration of wear surfaces due to limited oxidation</p>
	<p><b>630°C, 4,522 m – sample</b>  <i>(wear scar = 19 x 5 mm)</i>  Isolated areas of 'glaze' on asperities (raised areas) of limited transferred material</p>
	<p><b>750°C, 4,522 m – sample</b>  <i>(wear scar = 18 x 5 mm, also 690°C)</i>  Evidence of significant plastic deformation of the Incoloy MA956, 'glaze' build-up beginning to spread out from asperities</p>

**Fig. 7:** Optical Images for Incoloy MA956 versus Incoloy 800HT at 0.905 m.s<sup>-1</sup> (similar results at 0.654 m.s<sup>-1</sup>)



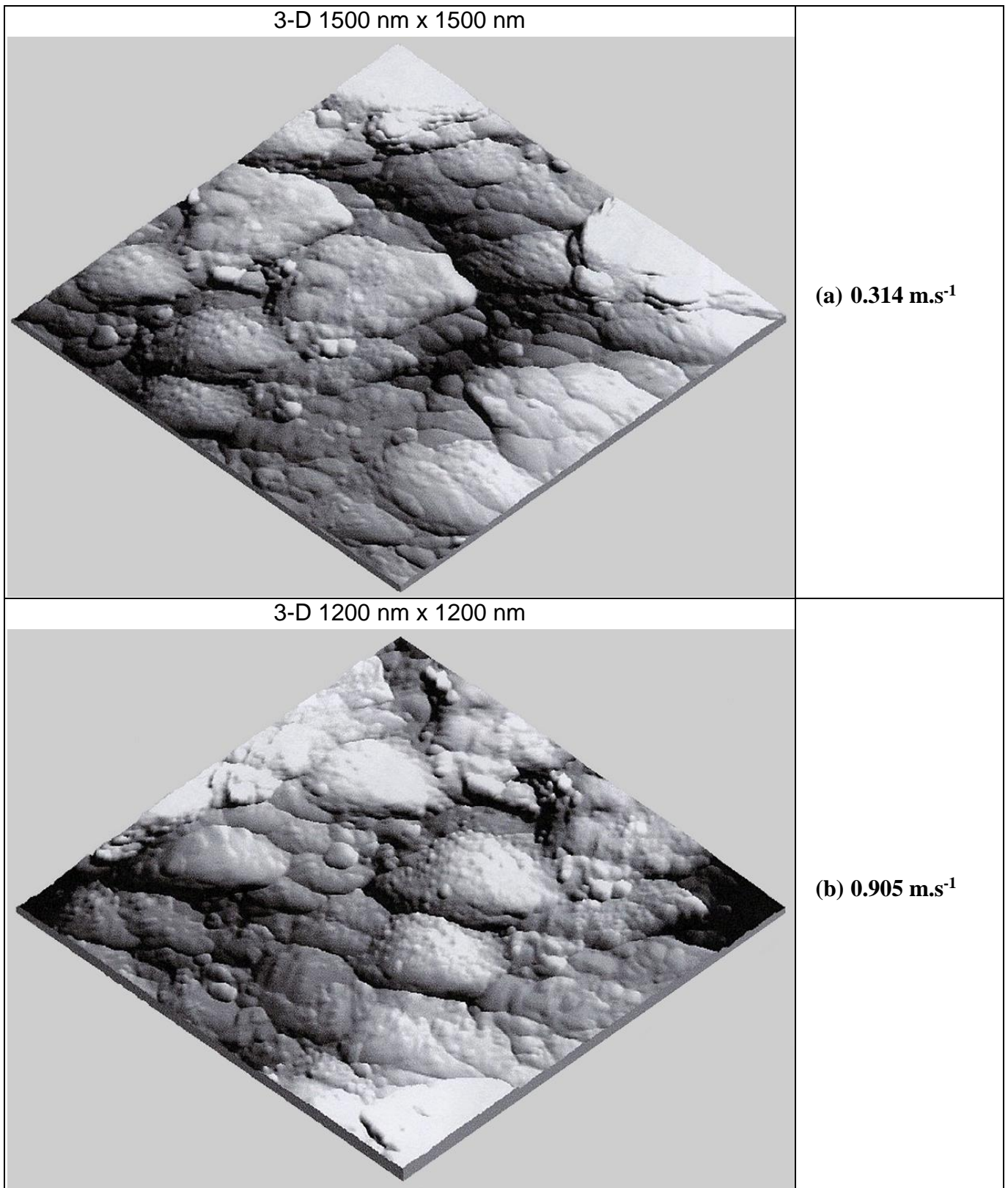
 <p>x300 0000 20kV 100µm</p>	<p>A. Room Temperature (shown), also 270°C</p> <p>Mechanically mixed metallic transfer layers covering most of Incoloy MA956 wear scar</p>
 <p>x300 0000 20kV 100µm</p>	<p>B. 510°C (shown), also 390, 450 and 570°C</p> <p>Deformed metal from 'severe wear' with patchy metallic transfer</p>
 <p>Exposed Incoloy MA956</p> <p>'Glaze'</p> <p>'Glaze'</p> <p>x300 0000 20kV 100µm</p>	<p>C. 630 (left) and 750°C (right), also 690°C</p> <p>'Glaze' formation in early stages at 630°C, more developed 'glaze' at 690 (not shown) and comprehensive development at 750°C</p>

**Fig. 8:** SEM micrographs for Incoloy MA956 versus Incoloy 800HT at 0.314 m.s<sup>-1</sup> – wear surfaces

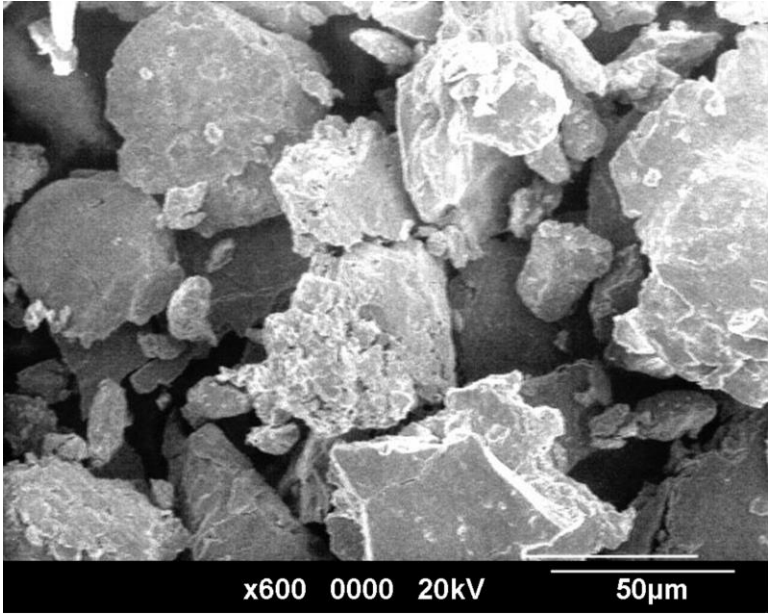
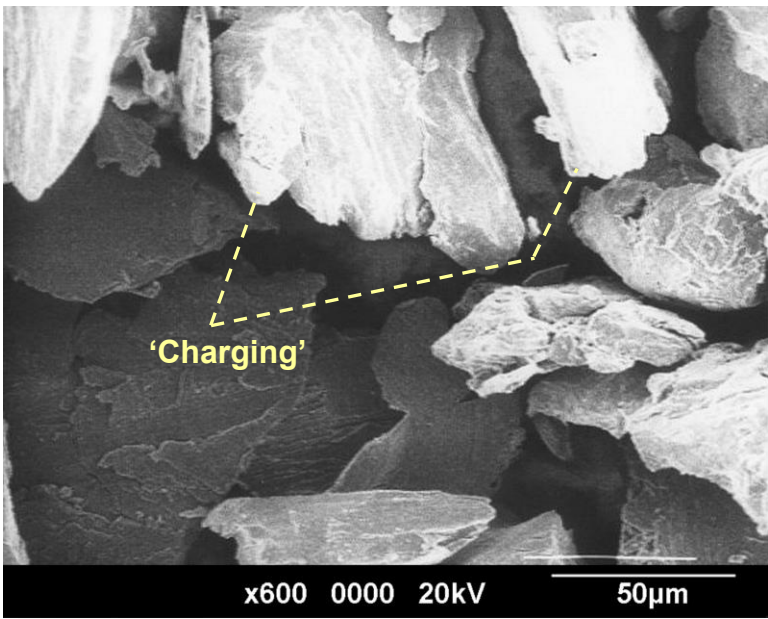
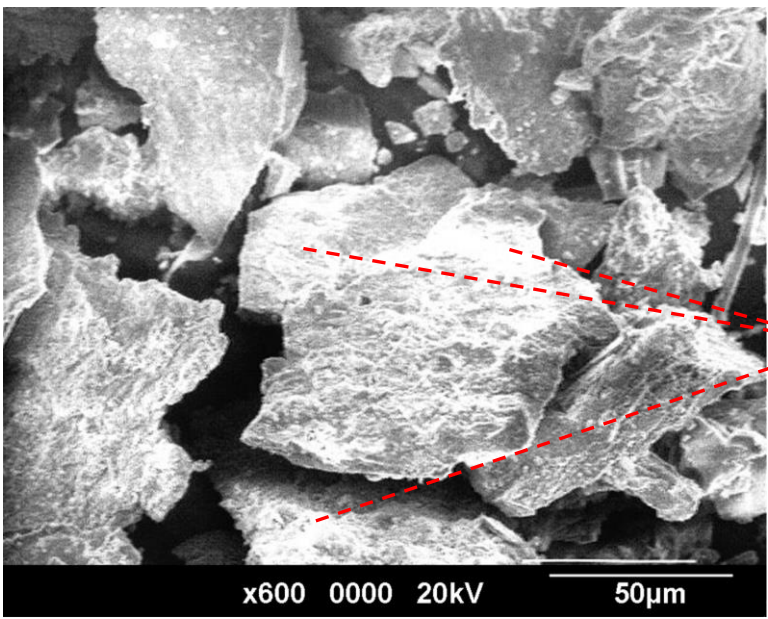
 <p data-bbox="384 663 831 696">x300 0000 20kV 100µm</p>	<p data-bbox="948 315 1442 383">A. Room Temperature (shown), also 270°C</p> <p data-bbox="995 398 1410 499">Mechanically mixed metallic transfer layers covering most of Incoloy MA956 wear scar</p>
 <p data-bbox="384 1328 831 1361">x300 0000 20kV 100µm</p>	<p data-bbox="948 943 1394 1010">B. 510°C (shown), also 390, 450, 570 and 630°C</p> <p data-bbox="995 1025 1442 1160">Deformed metal from 'severe wear' with limited metallic transfer (greater than at 0.314 m.s<sup>-1</sup>), odd patch of 'glaze' at 630°C only</p>
 <p data-bbox="384 1993 831 2027">x300 0000 20kV 100µm</p>	<p data-bbox="948 1581 1358 1615">C. 750°C (shown), also 690°C</p> <p data-bbox="995 1630 1426 1798">'Glaze' formation very patchy at 690°C (not shown), more developed 'glaze' but still patchy at 750°C and more fractured at 0.905 m.s<sup>-1</sup> than at 0.314 m.s<sup>-1</sup></p>

**Fig. 9:** SEM micrographs for Incoloy MA956 versus Incoloy 800HT at 0.905 m.s<sup>-1</sup> – wear surfaces



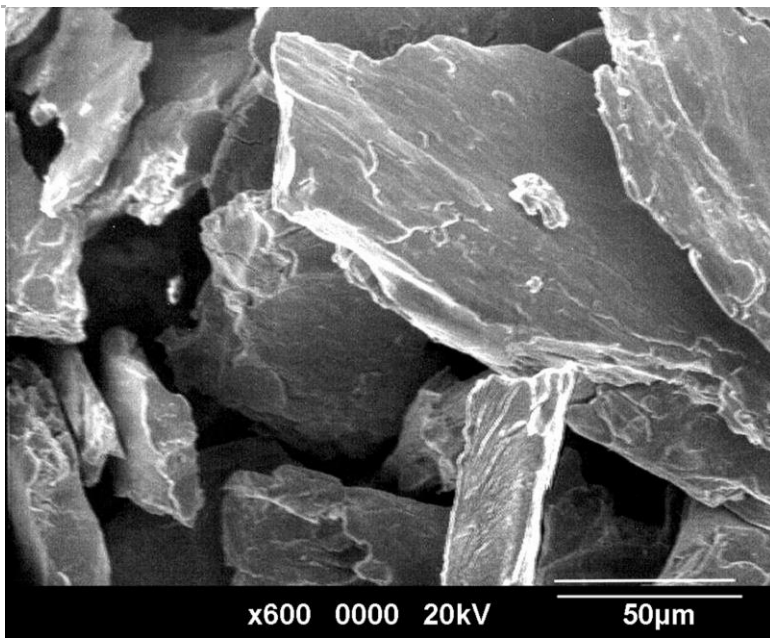


**Fig. 10: AFM image of ‘glaze’ layer surfaces produced on Incoloy MA956 (slid against Incoloy 800HT) at 750°C and sliding speeds of (a)  $0.314 \text{ m.s}^{-1}$  and (b)  $0.905 \text{ m.s}^{-1}$  [58]**

	<p>A. Room Temperature (shown), also 270°C</p> <p>Large, flat angular metallic particles of size between 20 <math>\mu\text{m}</math> and 1 mm</p>
	<p>B. 510°C (shown), also 390, 450 and 570°C</p> <p>Large, flat angular metallic particles of size between 20 <math>\mu\text{m}</math> and 1 mm</p> <p>Very fine oxide debris (&lt;1 <math>\mu\text{m}</math> in size) present in very low amounts from 390°C and increasing with rising temperature.</p> <p>'Charging' on debris due to the presence of oxide at 510°C</p>
	<p>C. 630 and 750°C (shown), also 690°C</p> <p>Large, flat angular metallic particles of size between 20 <math>\mu\text{m}</math> and 1 mm</p> <p>Very fine oxide debris (&lt;1 <math>\mu\text{m}</math> in size) present in significant amounts from 630°C upwards</p>

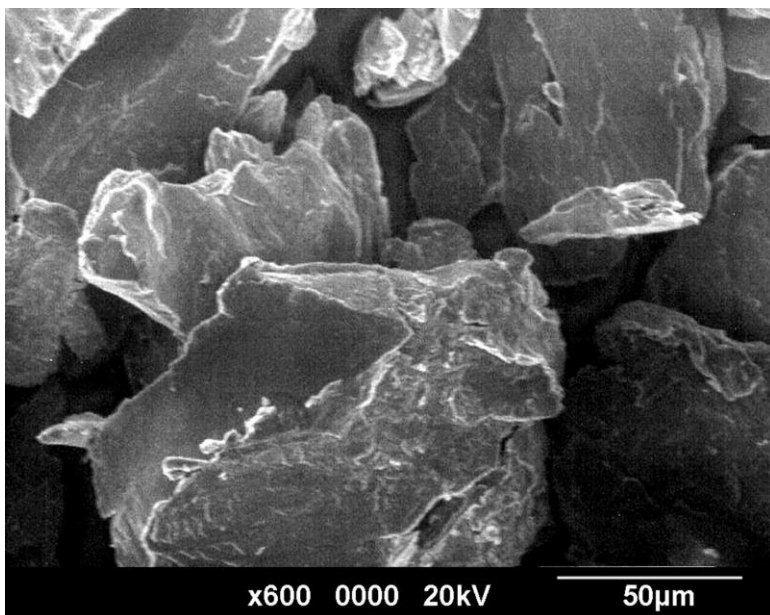
**Fig. 11:** SEM micrographs for Incoloy MA956 versus Incoloy 800HT at 0.314 m.s<sup>-1</sup> – debris





A. Room Temperature (shown), also 270°C

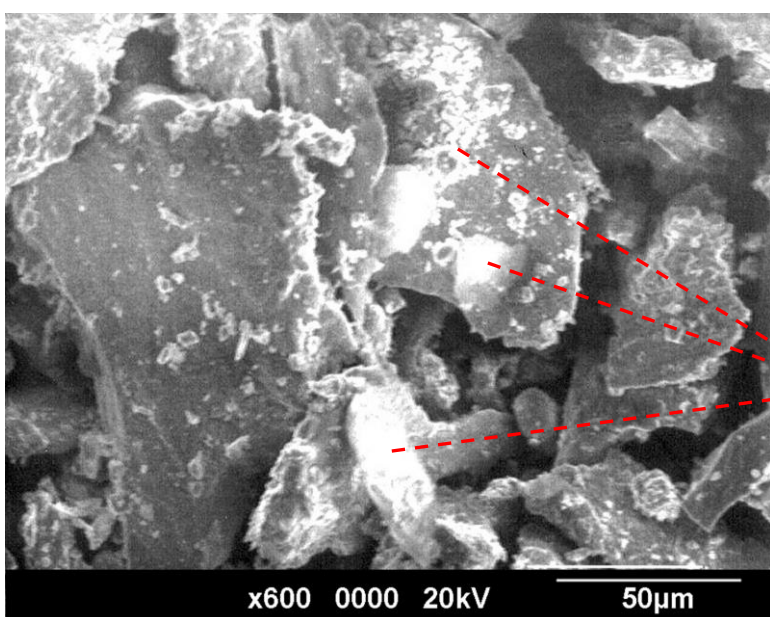
Large, flat angular metallic particles of size between 20  $\mu\text{m}$  and 1 mm



B. 510°C (shown), also 390, 450, 570 and 630°C

Large, flat angular metallic particles of size between 20  $\mu\text{m}$  and 1 mm

Very fine oxide debris (<1  $\mu\text{m}$  in size) present in very low amounts from 390°C and increasing with rising temperature (no charging at 510°C – less retained oxide).






C. 750°C (shown), also 690°C

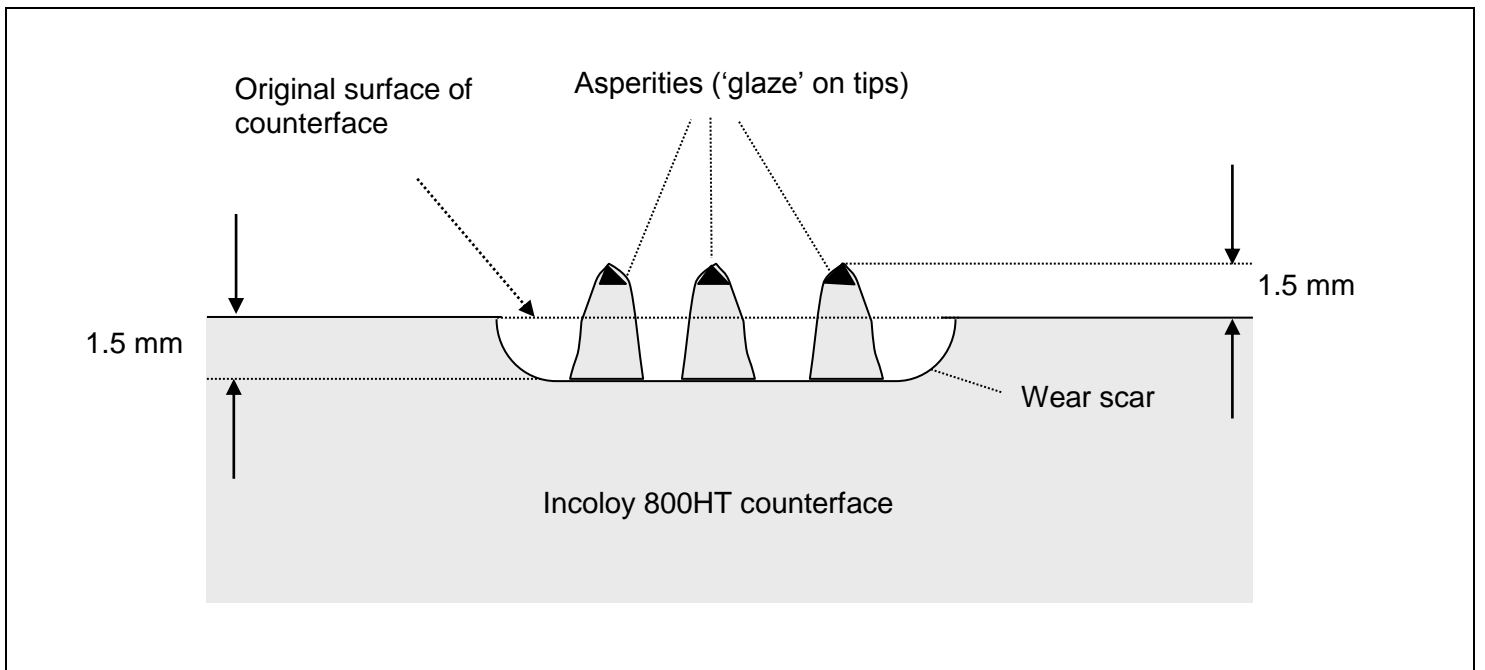
Large, flat angular metallic particles of size between 20  $\mu\text{m}$  and 1 mm

Increasing levels of very fine oxide debris (<1  $\mu\text{m}$  in size), present in significant amounts from 630°C upwards

**Fig. 12:** SEM micrographs for Incoloy MA956 versus Incoloy 800HT at 0.905  $\text{m}\cdot\text{s}^{-1}$  – debris

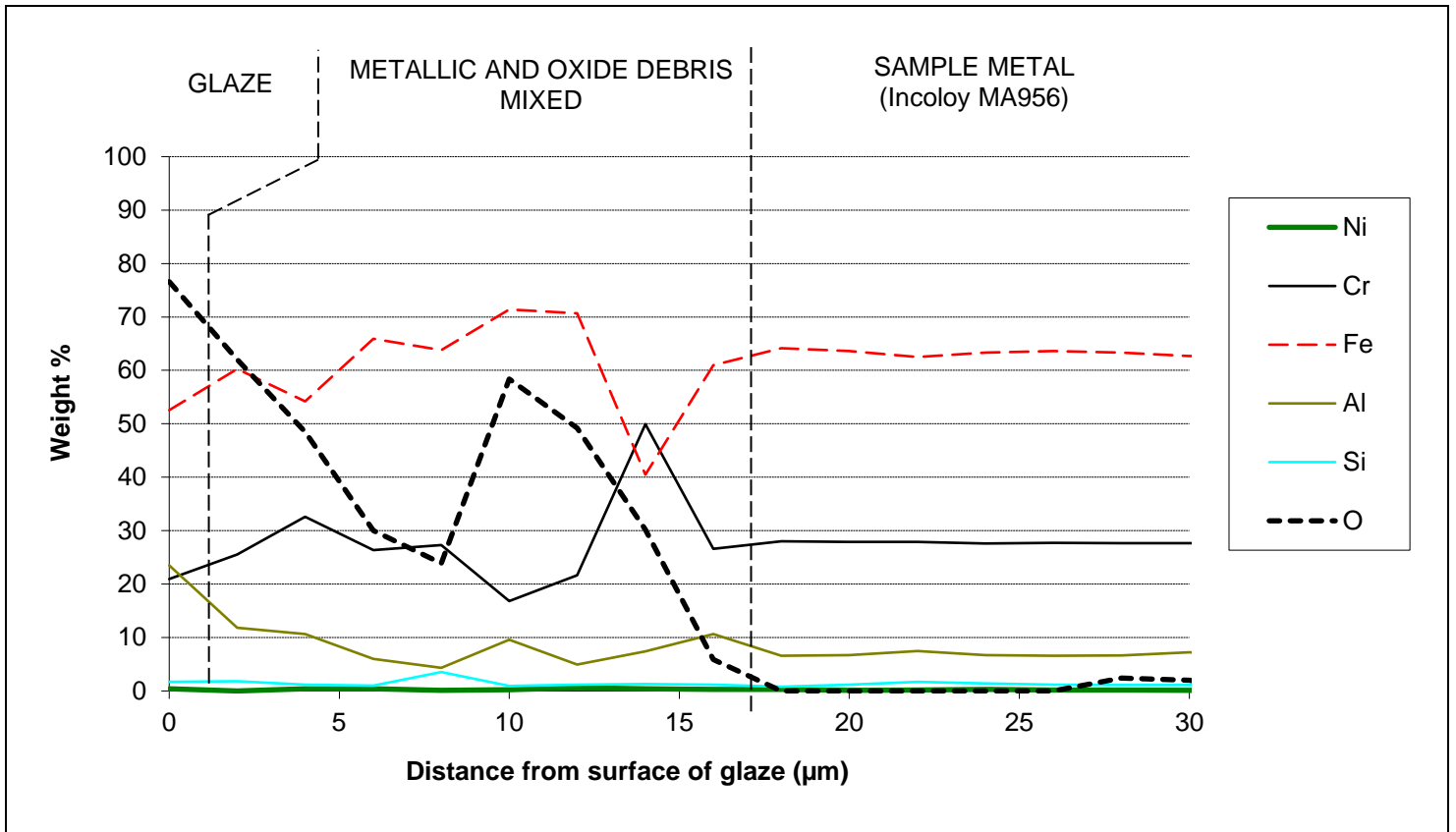
	<p><b>Room Temperature, 4,522 m – counterface</b>  <i>(section = 15 x 5 mm, representative up to 450°C)</i>          Highly worn wear scar with limited transfer layer</p>
	<p><b>570°C, 4,522 m – counterface</b>  <i>(section = 15 x 5 mm, applicable between 510°C and 630°C)</i>          Deeply grooved wear scar, 'glaze' free asperities formed due to transfer and / or back-transfer of metallic debris</p>
	<p><b>750°C, 4,522 m – counterface</b>  <i>(section = 15 x 5 mm, also applicable at 690°C)</i>          Deeply grooved wear scar, 'glaze' forming only on tops of transferred / back-transferred asperities with slightly fewer asperities at 0.905 m.s<sup>-1</sup></p>

(a) Counterface wear scar optical images

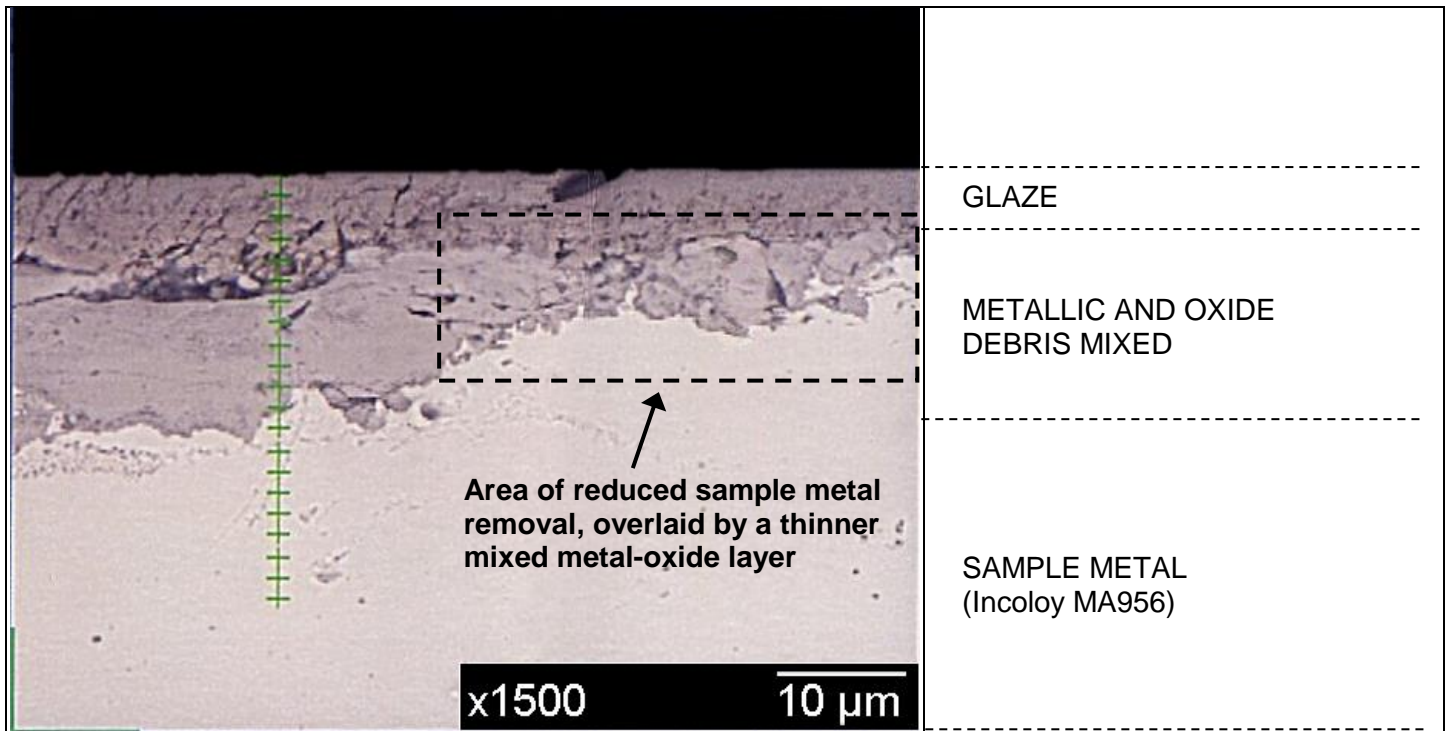


(b) Counterface wear scar cross-section schematic

**Fig. 13:** (a) Incoloy 800HT counterface wear scar optical images (shown optical images from 0.314 m.s<sup>-1</sup>, near-identical observations at 0.654 and 0.905 m.s<sup>-1</sup>) and (b) counterface wear scar cross-section schematic for 0.314, 0.654 and 0.905 m.s<sup>-1</sup>, worn against an Incoloy MA956 sample



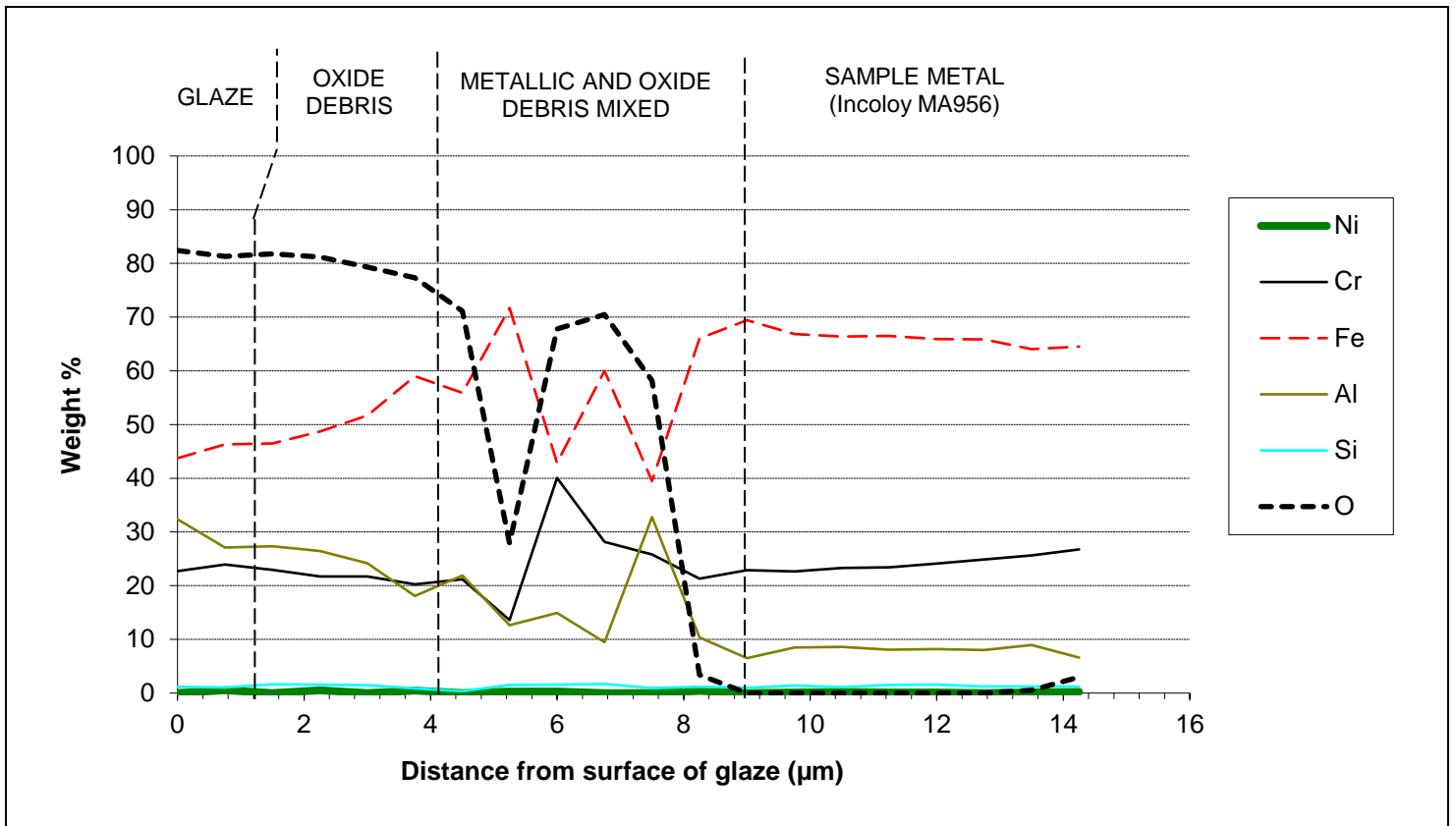
(a) Autopoint EDX



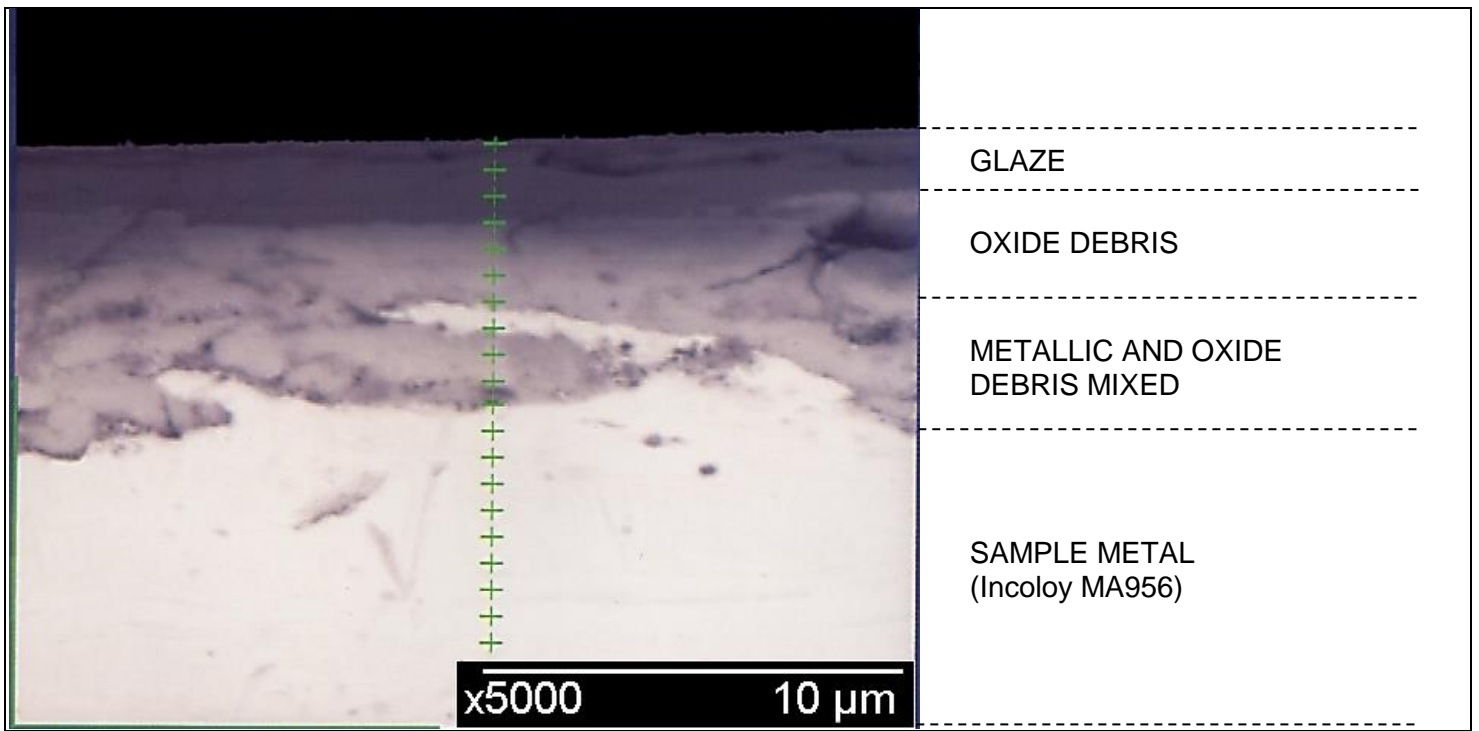
(b) Cross-section

**Fig. 14:** Data from Autopoint EDX analysis for Incoloy MA956 versus Incoloy 800HT, sliding speed  $0.314 \text{ m}\cdot\text{s}^{-1}$ , temperature  $750^\circ\text{C}$  (amounts of each substance present expressed as percentage of non-O content; amount of O expressed as percentage of overall content; dividing lines between different layers based on SEM observations and are average values), alongside representative cross-sections through which Autopoint EDX measurements were taken





(a) Autopoint EDX



(b) Cross-section

**Fig. 15:** Data from Autopoint EDX analysis for Incoloy MA956 versus Incoloy 800HT, sliding speed  $0.905 \text{ m}\cdot\text{s}^{-1}$ , temperature  $750^\circ\text{C}$  (amounts of each substance present expressed as percentage of non-O content; amount of O expressed as percentage of overall content; dividing lines between different layers based on SEM observations and are average values), alongside representative cross-sections through which Autopoint EDX measurements were taken

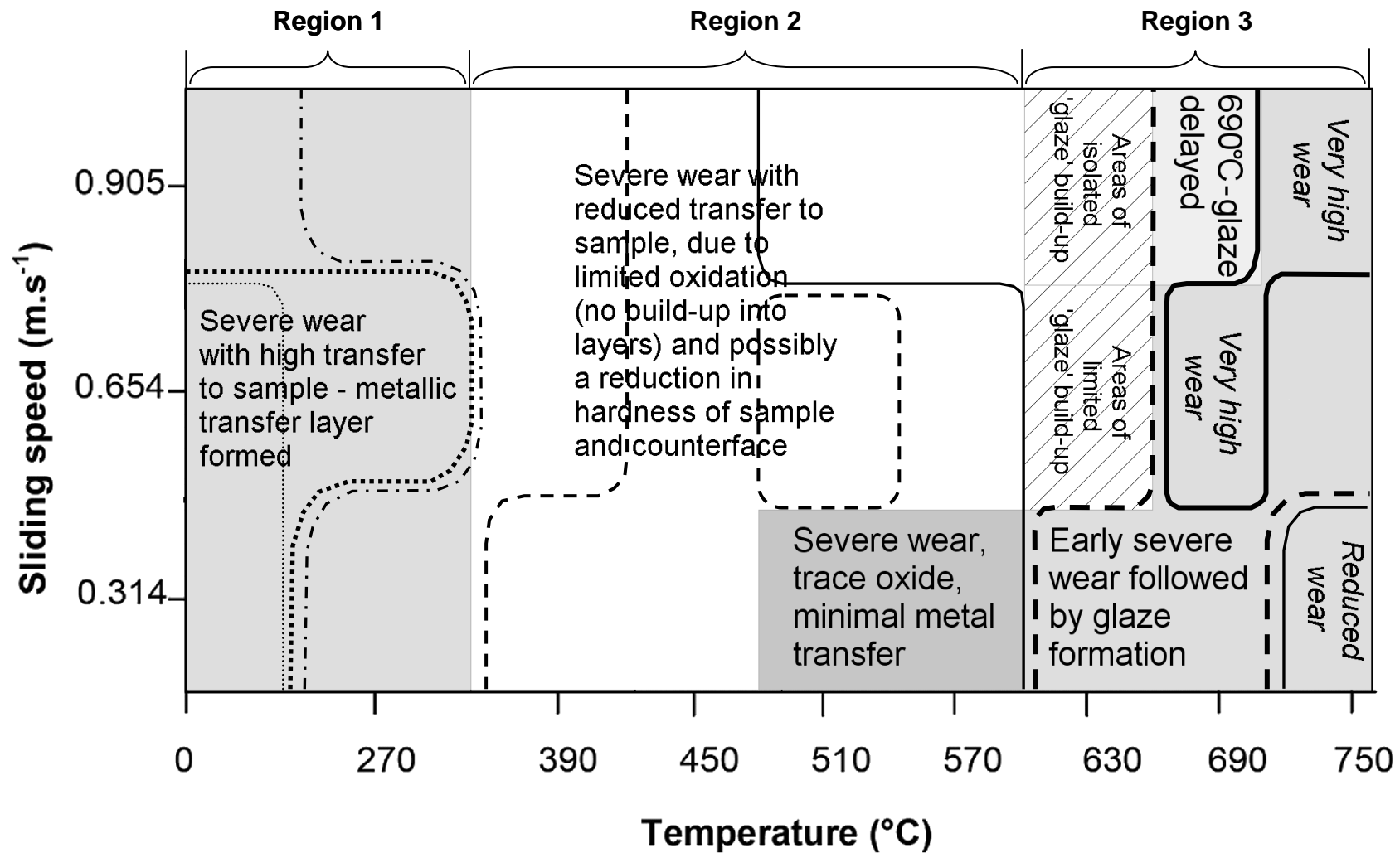
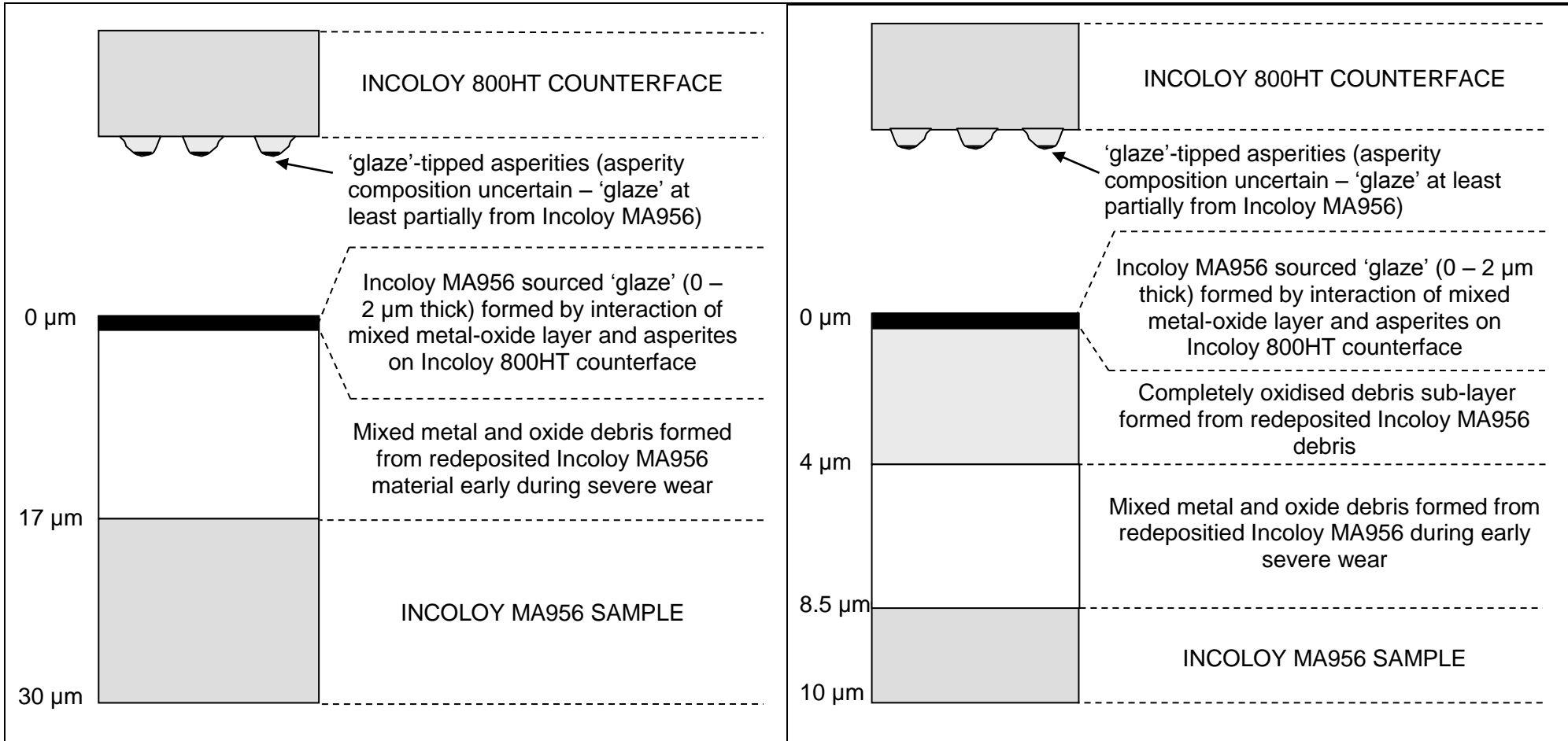


**Fig. 16:** Wear map for Incoloy MA956 versus Incoloy 800HT between 630°C and 750°C (load = 7N), with weight loss (contour) data superimposed; the different areas of shading denote the range of conditions over which the various detailed wear conditions were observed



(a) 0.314 m.s<sup>-1</sup>

(b) 0.905 m.s<sup>-1</sup>

**Fig. 17:** Layers formed on Incoloy MA956 sample and Incoloy 800HT counterface at 750°C



	Fe	Ni	Cr	Al	Ti	Mn	W	Co	Si	C
<b>Incoloy MA956</b>	74	-	20	4.5	0.5	0.05	-	-	-	-
<b>Incoloy 800HT</b>	43.8	32.5	21.0	0.37	0.37	1.5 max	-	-	0.4	0.1 max

**Table 1:** Nominal compositions of alloys (wt%)

Sliding speed (m.s <sup>-1</sup> )	Temperature (°C)										
	R.T.	270	390	450	510	570	630	690	750		
<b>0.905</b>	FeCr + Cr <sub>0.19</sub> Fe <sub>0.7</sub> Ni <sub>0.11</sub>  (extended transfer layers)		FeCr only  (reduced transfer layers)				FeCr + Cr <sub>1.3</sub> Fe <sub>0.7</sub> O <sub>3</sub>  (‘glaze’ present)				
<b>0.654</b>											
<b>0.314</b>			FeCr + Cr <sub>1.3</sub> Fe <sub>0.7</sub> O <sub>3</sub> (no ‘glaze’)								

**Table 2:** X-Ray diffraction data for Incoloy MA956 versus Incoloy 800HT between room temperature and 750°C (load = 7N); sliding speed presented in reverse order to match the wear map presented in Fig. 16.

Room temp. / 0.314 m.s <sup>-1</sup>		Room temp. / 0.905 m.s <sup>-1</sup>	
6.313	<b>Mean = 5.82 GPa</b>	6.334	<b>Mean = 6.72 GPa</b>
4.429		6.647	
6.377		6.647	
5.963		7.086	
6.042		6.861	
270°C / 0.314 m.s <sup>-1</sup>		270°C / 0.905 m.s <sup>-1</sup>	
5.447	<b>Mean = 7.11 GPa</b>	6.144	<b>Mean = 6.10 GPa</b>
8.765		6.228	
4.651		6.249	
7.829		5.924	
8.836		5.943	

(Mean hardness of unworn Incoloy MA956 (sample) = 4.129 GPa,  
mean hardness of unworn Incoloy 800HT (counterface) = 2.15 GPa)

**Table 3:** Hardness data for transfer layers at room temperature and 270°C, Incoloy MA956 versus Incoloy 800HT (load = 7N, sliding distance = 4,522 m, hardness values in GPa, Vickers micro-indenter - 50g, sample size = 5)

Unworn substrate (preheated to 750°C for 4 hours)		'Glaze' formed at 0.314 m.s <sup>-1</sup>		'Glaze' formed at 0.905 m.s <sup>-1</sup>	
4.478	<b>Mean = 4.129 GPa</b>	6.110	<b>Mean = 9.63 GPa</b>	19.667	<b>Mean = 21.26 GPa</b>
3.667		7.185		35.659	
3.910		11.743		9.373	
4.237		11.611		17.542	
4.355		11.481		24.044	

**Table 4:** Hardness data for 'glaze' and undeformed substrate, Incoloy MA956 versus Incoloy 800HT slid at 750°C (load = 7N, sliding distance = 4,522 m, hardness values in GPa, Vickers micro-indenter - 50g, sample size = 5)

Temperature (°C)	30	150	270	390	450	510
<b>Incoloy MA956</b>	1.99	1.71	1.45	1.24	1.16	0.97
<b>Incoloy 800HT</b>	3.38	2.16	1.68	1.52	1.34	0.55

**Table 5:** Mean Knoop hardness (hot hardness, 50 g load, 12 s dwell time) of Incoloy MA956 and Incoloy 800HT between room temperature to 510°C [9]